

DR. ATHANASIOS PASCHALIS (Orcid ID : 0000-0003-4833-9962)

DR. MARTIN GERARD DE KAUWE (Orcid ID : 0000-0002-3399-9098)

DR. PAUL HANSON (Orcid ID : 0000-0001-7293-3561)

DR. WEI LI (Orcid ID : 0000-0003-2543-2558)

DR. YIQI LUO (Orcid ID : 0000-0002-4556-0218)

PROF. JOSEP PENUELAS (Orcid ID : 0000-0002-7215-0150)

DR. JULIA PONGRATZ (Orcid ID : 0000-0003-0372-3960)

DR. SARA VICCA (Orcid ID : 0000-0001-9812-5837)

MR. DONGHAI WU (Orcid ID : 0000-0002-4638-3743)

Article type : Primary Research Articles

Rainfall-manipulation experiments as simulated by terrestrial biosphere models: where do we stand?

Athanasios Paschalis ^{1*}, Simone Fatichi ², Jakob Zscheischler ^{3,4}, Philippe Ciais ⁵, Michael Bahn ⁶, Lena Boysen ⁷, Jinfeng Chang ⁵, Martin De Kauwe ⁸, Marc Estiarte ^{9,10}, Daniel Goll ^{5,11}, Paul J. Hanson ¹², Anna B. Harper ¹³, Enqing Hou ¹⁴, Jaime Kigel ¹⁵, Alan K. Knapp ¹⁶, Klaus Steenberg Larsen ¹⁷, Wei Li ^{5,18}, Sebastian Lienert ^{3,4}, Yiqi Luo ¹⁴, Patrick Meir ¹⁹, Julia E. M. S. Nabel ⁷, Romà Ogaya ^{9,10}, Anthony J Parolari ²¹, Changhui Peng ²², Josep Peñuelas ^{9,10}, Julia Pongratz ²³, Serge Rambal ^{9,10}, Inger Kappel Schmidt ¹⁷, Hao Shi ²⁴, Marcelo Sternberg

This article has been accepted for publication and undergone full peer review but has not been through the copyediting, typesetting, pagination and proofreading process, which may lead to differences between this version and the [Version of Record](#). Please cite this article as [doi: 10.1111/GCB.15024](https://doi.org/10.1111/GCB.15024)

This article is protected by copyright. All rights reserved

²⁵, Hanqin Tian ²⁴, Elisabeth Tschumi ^{3,4}, Anna Ukkola ⁸, Sara Vicca ²⁶, Nicolas Viovy ⁵, Ying-Ping Wang ²⁷, Zhuonan Wang ²⁴, Karina Williams ²⁸, Donghai Wu ²⁹, Qiuhan Zhu ³⁰

¹ *Department of Civil and Environmental Engineering, Imperial College London, UK*

² *Institute of Environmental Engineering, ETH Zurich, Switzerland*

³ *Climate and Environmental Physics, University of Bern, Switzerland;*

⁴ *Oeschger Centre for Climate Change Research, University of Bern, Bern, Switzerland*

⁵ *Laboratoire des Sciences du Climat et de l'Environnement, Gif sur Yvette, France*

⁶ *Department of Ecology, University of Innsbruck, Austria*

⁷ *Max Planck Institute for Meteorology, Hamburg, Germany*

⁸ *ARC Centre of Excellence for Climate Extremes, University of New South Wales, Sydney, NSW, Australia*

⁹ *CSIC, Global Ecology Unit CREAF-CSIC-UAB, 08193 Bellaterra, Catalonia, Spain*

¹⁰ *CREAF, 08193 Cerdanyola del Vallès, Catalonia, Spain*

¹¹ *Department of Geography, University of Augsburg, Germany*

¹² *Environmental Sciences Division, Oak Ridge National Laboratory, Oak Ridge, TN, USA*

¹³ *Department of Mathematics, University of Exeter, Exeter, UK*

¹⁴ *Department of Biological Sciences, Northern Arizona University*

¹⁵ *Institute for Plant Sciences and Genetics, Faculty of Agriculture, Food and Environment, The Hebrew University of Jerusalem, Rehovot Campus, Israel*

¹⁶ *Graduate Degree Program in Ecology, Department of Biology, Colorado State University*

¹⁷ *Dept. of Geosciences and Natural Resource Management, University of Copenhagen, Rolighedsvej 23, 1958 Frederiksberg C, Denmark*

¹⁸ *Ministry of Education Key Laboratory for Earth System modeling, Department of Earth System Science, Tsinghua University, Beijing 100084, China*

¹⁹ *Research School of Biology, Australian National University, Australia*

²⁰ *School of Geosciences, University of Edinburgh, United Kingdom*

²¹ *Department of Civil, Construction, and Environmental Engineering, Marquette University, Milwaukee, WI, USA*

²² *Department of Biology Sciences, University of Quebec at Montreal, Canada*

²³ *Department of Geography, Ludwig Maximilian University of Munich, Germany*

²⁴ *International Center for Climate and Global Change Research, School of Forestry and Wildlife Sciences, Auburn University, Auburn, USA.*

²⁵ *School of Plant Sciences and Food Security, Faculty of Life Sciences, Tel Aviv University, Tel Aviv 69978, Israel*

²⁶ *Centre of Excellence PLECO (Plants and Ecosystems), Biology Department, University of Antwerp, Belgium*

²⁷ *CSIRO Marine and Atmospheric Research and Centre for Australian Weather and Climate Research*

²⁸ *Met Office Hadley Centre, FitzRoy Road, Exeter EX1 3PB, Devon, UK*

²⁹ *Sino-French Institute for Earth System Science, College of Urban and Environmental Sciences, Peking University*

³⁰ *Center for Ecological Forecasting and Global Change, College of Forestry, Northwest A&F University, China*

**Corresponding Author: a.paschalis@imperial.ac.uk, +44 (0)207 594 6004*

1 **Abstract**

2 Changes in rainfall amounts and patterns have been observed and are expected to continue in the near future
3 with potentially significant ecological and societal consequences. Modelling vegetation responses to changes in
4 rainfall is thus crucial to project water and carbon cycles in the future. In this study, we present the results of a
5 new model-data intercomparison project, where we tested the ability of ten terrestrial biosphere models to
6 reproduce observed sensitivity of ecosystem productivity to rainfall changes at ten sites across the globe, in
7 nine of which, rainfall exclusion and/or irrigation experiments had been performed.

8 The key results are:

9 (a) Inter-model variation is generally large and model agreement varies with time scales. In severely water
10 limited sites, models only agree on the interannual variability of evapotranspiration and to a smaller extent
11 gross primary productivity. In more mesic sites model agreement for both water and carbon fluxes is typically
12 higher on fine (daily-monthly) time scales and reduces on longer (seasonal-annual) scales.

13 (b) Models on average overestimate the relationship between ecosystem productivity and mean rainfall
14 amounts across sites (in space) and have a low capacity in reproducing the temporal (interannual) sensitivity of
15 vegetation productivity to annual rainfall at a given site, even though observation uncertainty is comparable to
16 inter-model variability.

17 (c) Most models reproduced the sign of the observed patterns in productivity changes in rainfall manipulation
18 experiments but had a low capacity in reproducing the observed magnitude of productivity changes. Models
19 better reproduced the observed productivity responses due to rainfall exclusion than addition.

20 (d) All models attribute ecosystem productivity changes to the intensity of vegetation stress and peak leaf area,
21 whereas the impact of the change in growing season length is negligible. The relative contribution of the peak
22 leaf area and vegetation stress intensity was highly variable among models.

23 **Keywords:** drought, irrigation, terrestrial biosphere models, rainfall manipulation experiment

24 **1 Introduction**

25 Understanding the impact of rainfall changes on ecosystem functioning and vegetation dynamics is crucial for
26 accurately predicting responses of vegetation structure, composition and dynamics under present or future
27 conditions. Changes in both rainfall intensity and variability have been measured in the last decades
28 (Trenberth, 2011; IPCC, 2013). Changes in precipitation extremes have also been observed (Alexander *et al.*,
29 2006) and according to climate model projections, such changes will intensify as we progress through the 21st
30 century (IPCC, 2012; Knutti and Sedláček, 2013).

31 Changes in rainfall can affect energy and carbon fluxes at the land surface (Green *et al.*, 2017). Rainfall
32 changes modify soil water dynamics, alter plant water status and consequently the terrestrial biogeochemical
33 cycles (Heisler-White, *et al.*, 2008; Allan *et al.*, 2014) through changes in plant productivity or plant mortality
34 (Allen, *et al.*, 2015). The importance of plant water limitation has been highlighted by the fact that semi-arid
35 regions, which typically experience drought, control part of the global interannual variability of the terrestrial
36 carbon sink (Ahlström *et al.*, 2015), with an increasing sensitivity during the last decades (Poulter *et al.*, 2014).
37 The importance of water limitation on carbon fluxes will likely increase soon, since terrestrial vegetation is
38 thought to operate close to its critical hydraulic thresholds across a wide range of ecosystems (Choat *et al.*,
39 2012), even though the full implications of this result are still debated (Klein *et al.*, 2014; Körner, 2019). As a
40 direct consequence, minor changes in plant water availability worldwide can lead to significant impacts on the
41 terrestrial carbon sink (Allen *et al.*, 2010; Zhao and Running, 2010; Reichstein *et al.*, 2013; Frank *et al.*, 2015;
42 Humphrey *et al.*, 2018; Green *et al.*, 2019).

43 To understand the ecosystem responses to changes in rainfall amounts and patterns at the local scale, rainfall
44 manipulations experiments have been conducted. Typically, such experiments change the overall rainfall
45 amount by exclusion (Estiarte *et al.*, 2016; Martin-Stpaul *et al.*, 2013; Limousin *et al.*, 2009) or irrigation
46 (Collins *et al.*, 2012) and responses are commonly quantified by changes in Aboveground Net Primary
47 Production (ANPP). In some experiments such as the Amazon rainfall exclusion experiment, (Nepstad *et al.*,
48 2007) additional detailed data quantifying changes in forest structure and composition have been obtained.
49 There are a small number of experiments where the structure of rainfall pulses is modified e.g. (Fay *et al.*,
50 2008; Heisler-White, *et al.*, 2008; Vicca *et al.*, 2014). Rainfall manipulation experiments have been conducted
51 in a range of ecosystems, spanning from semiarid shrublands (Báez *et al.*, 2013), to temperate (Hanson and
52 Wullschleger, 2003) and tropical forests (Fisher *et al.*, 2007; Nepstad *et al.*, 2007), even though most of the
53 experiments have focused on grasslands or low-stature vegetation due to the difficulties in setting up
54 experiments. Those experiments have identified a strong correlation between rainfall changes and vegetation

55 productivity (e.g. Heisler-White *et al.*, 2009; Stuart-Haëntjens *et al.*, 2018), phenology (e.g. Peñuelas *et al.*,
56 2004), plant community structure e.g. (Miranda *et al.*, 2011; Zhang *et al.*, 2019) and belowground carbon
57 dynamics e.g. (Vicca *et al.*, 2014; Hagedorn *et al.*, 2016; Hasibeder *et al.*, 2015). Despite the important findings
58 derived from these field experiments, these studies have strong spatial and temporal limitations; they reported
59 only few variables and it is challenging to extrapolate information beyond the specific design of the
60 experiment. Extrapolation and mechanistic understanding related to vegetation responses to changes in
61 precipitation can be better achieved by combining model and data driven approaches (e.g. Kayler *et al.*, 2015).

62 Modelling vegetation responses to changes in water availability is a challenging task (Xu *et al.*, 2013). Despite
63 strong evidence that modelling responses to drought is a significant factor affecting terrestrial carbon dynamics
64 (Trugman *et al.*, 2018), a commonly accepted parameterization of water limitation does not exist (Egea, *et al.*,
65 2011; Zhou *et al.*, 2013; Fatichi, *et al.*, 2016; Medlyn, *et al.*, 2016a; Hu *et al.*, 2018). Plant water stress
66 simulated in terrestrial biosphere models can affect various processes but is commonly a function of either
67 volumetric soil water content e.g. (Clark *et al.*, 2011) or soil water potential e.g. (Fatichi, *et al.*, 2012; Manzoni
68 *et al.*, 2013; Lawrence *et al.*, 2019), integrated over the root zone. Examples of how water limitation affects
69 plant functions include a decline in stomatal conductance affecting photosynthesis (Egea, *et al.*, 2011; Fatichi,
70 *et al.*, 2012; De Kauwe, *et al.*, 2015), changes in the photosynthetic parameters V_{cmax} and J_{max} e.g. (Krisner *et*
71 *al.*, 2005), and/or accelerated senescence of plant tissues, especially leaves (Thurner *et al.*, 2017) leading to
72 drought-induced deciduousness. Recently, significant efforts have been made to include more detailed plant
73 hydraulics, to better describe water flow within the soil-plant-water continuum (Bonan *et al.*, 2014;
74 Mirfenderesgi *et al.*, 2016; Eller *et al.*, 2018; Kennedy *et al.*, 2019; Lawrence *et al.*, 2019) and to include
75 dynamics of non-structural carbohydrates to simulate consequences of water stress for carbon allocation and
76 carbon starvation (reviewed in Fatichi *et al.*, 2019).

77 A large discrepancy of predicted model responses has direct consequences for the uncertainties related to the
78 fate of terrestrial carbon under a changing climate (Zscheischler, *et al.*, 2014b; Ahlström *et al.*, 2015;
79 Humphrey *et al.*, 2018). This is the case because the terrestrial vegetation and thus the terrestrial land carbon
80 sink introduces the largest uncertainties of the global carbon cycle (Le Quéré *et al.*, 2018). In this context, large
81 epistemic model uncertainties can have considerable impacts on our ability to forecast the growth rate of
82 atmospheric CO₂. Additionally, vegetation responses to water stress can influence land-atmosphere coupling
83 (Koster, 2004; Seneviratne *et al.*, 2013; Lemordant *et al.*, 2016; Gentine *et al.*, 2019), since vegetation cover
84 and canopy conductance affect land surface energy balance. This will have a large impact on our skill to model

85 the coupled hydrological, plant physiological and meteorological processes and thus robustly projecting
86 climate change (Miralles *et al.*, 2018).

87 To reduce this source of epistemic uncertainty and understand the reasons for model disagreement, a detailed
88 comparison between the responses of different modelling schemes with respect to plant water availability is
89 essential. Rainfall manipulation experiments assessing vegetation responses to water limitation are particularly
90 useful in this regard. Arguably, this is an extremely important test to evaluate the structure and parameter
91 values of a model and its capability to reproduce responses to environmental changes. A model should be able
92 to reproduce the observed dynamics under control and manipulated conditions in order to be considered robust,
93 especially for climate change simulations (Medlyn *et al.*, 2015). Despite the importance of this comparison,
94 there are only few examples that have compared terrestrial biosphere models and global change manipulation
95 experiments (De Kauwe *et al.*, 2013, 2017; Fatichi and Leuzinger, 2013; Powell *et al.*, 2013; Zaehle *et al.*,
96 2014; Medlyn *et al.*, 2015). Recently, Wu *et al.* (2018) compared 14 models under different idealized rainfall
97 scenarios for three grassland experiments sites and showed a fair reproduction of spatial sensitivities of ANPP
98 to rainfall but large differences in the modelled asymmetric response of ANPP to interannual i.e. temporal
99 rainfall variability at a given site. Wu *et al.* (2018) were not able to evaluate the modelled responses with
100 respect to actual experiments because they used idealized rainfall changes that did not exactly mimic the site
101 treatments. In this study we perform such an evaluation. We make use of ten sites with diverse climates and
102 biomes, where multi-year rainfall manipulation experiments took place to evaluate ten terrestrial biosphere
103 models, representing an unprecedented data-model intercomparison effort focused on ecosystem responses to
104 water limitation. This data-model intercomparison will address the following questions: (a) Can models
105 reproduce the observed responses to precipitation variability at rainfall manipulation sites? (b) Do models
106 accurately reproduce the spatial (across-sites) and temporal (within-site) dependence of vegetation productivity
107 to precipitation? (c) Which are the underlying reasons for model disagreement? Answering those questions will
108 provide insights on the robustness of Earth System model projections with respect to the global carbon cycle.

109 **2 Data and Methods**

110 **2.1 Sites**

111 Ten different sites with contrasted climates and biomes and sufficiently long records were considered here. For
112 all analyses presented in this study, the sites are termed: Lahav, Matta, SGS, Prades, Garraf, Konza
113 (AmeriFlux ID: US-Kon), Puèchabon (FluxNet ID: FR-Pue), Brandbjerg, Walker Branch (Walker Branch;
114 AmeriFlux ID: US-WBW) and Stubai (Table 1). The sites are in ascending order in terms of wetness index *WI*

115 defined as the average ratio of annual precipitation to annual potential evapotranspiration during the study
 116 period. For our analysis the sites are split in three wetness categories ($WI < 0.4$ [Lahav, Matta, SGS];
 117 $0.4 \leq WI < 1$ [Prades, Garraf, Konza, Puèchabon]; $WI \geq 1$ [Brandbjerg, Walker Branch, Stubai]).

118 The sites are in the USA (Konza, SGS, Walker Branch), Israel (Lahav, Matta), Spain (Garraf), France (Prades,
 119 Puèchabon), Austria (Stubai) and Denmark (Brandbjerg) and span a precipitation gradient from 253-1440 mm
 120 y^{-1} and include grasslands shrublands and forested ecosystems (Table 1). In eight sites rainfall exclusion
 121 experiments were carried out, and in four irrigation experiments. The experiment duration considered in this
 122 study was from 5 up to 32 years. The average experiment duration was 13.3 years.

123

124

Table 1: Site Description

Site	Lon/Lat	annual T [°C]	annual P [mm]	WI	Altitude [m]	Species	Soil Type	Drought Treatment	Irrigation Treatment	Years	Key References
Lahav	34.9/31.38	19.1	253	0.19	590	Annual grasses and shrubs, mostly <i>Sarcopoterium spinosum</i>	22.6% Sand, 39.7% Silt, 37.7% Clay	-30% rainfall for the entire year	+30% rainfall for the entire year	2002-2014	Tielbörger <i>et al.</i> , 2014
Matta	35.07/31.71	17.94	498	0.33	620	Similar to Lahav	19% Sand, 29.2% Silt, 51.8% Clay	-30% rainfall for the entire year	+30% rainfall for the entire year	2002-2014	Tielbörger <i>et al.</i> , 2014
SGS	-104.75/40.81	8.4	304	0.35	1650	C4 grasses, primarily (<i>Bouteloua gracilis</i> (H.B.K.) Lag. Ex Steud., <i>Buchloe dactyloides</i> (Nutt) Engelm., mixed with varying amounts of C3 grasses, cactus, shrubs and forb.	14% Sand, 58% Silt, 28% Clay	None	None	1986-2009	Heisler-White <i>et al.</i> , 2009
Prades	0.91/41.21	11.43	522	0.4	950	Mixed composition of <i>Quercus ilex</i> L., <i>Phillyrea latifolia</i> L., <i>Arbutus unedo</i> L., <i>Erica arborea</i> L., <i>Juniperus oxycedrus</i> L., <i>Cistus albidus</i> L. <i>Sorbus torminalis</i> (L.) Crantz and	48% Sand, 32% Silt and 20% Clay	-20% rainfall for the entire year	None	1999-2012	Ogaya and Peñuelas, 2007

						Acer monspessulanum L.						
Garraf	1.82/ 41.3	15.04	580	0.48	210	Erica multiflora, Globularia alypum	41% Sand, 39% Silt and 18% Clay,	-50% in spring and fall	None	2000- 2004	Beier <i>et al.</i> , 2009	
Konza	-96.6/ 39.1	12.8	830	0.7	342	Mixed C3(Solidago canadensis, Aster ericoides, Salix missouriensis) C4(Andropogon gerardii, Sorghastrum nutans, Panicum virgatum) Grassland	10% Sand, 35% Clay	None	irrigation +20% was provided at two sites termed lowland and upland	1982- 2013	Collins <i>et al.</i> , 2012	
Puèchabon	43.74/3.6	13.8	969	0.87	270	Overstory (Quercus ilex); Understory (Buxus sempervirens, Phyllirea latifolia, Pistacia terebinthus and Juniperus oxycedrus)	26% Sand, 35% Silt,39% Clay	-30% throughfall exclusion for the entire year	None	2004- 2013	Limousin <i>et al.</i> , 2009	
Brandbjerg	11.97/55.89	9.59	757	1.1	39	70% grasses (mostly Deschampsia flexuosa); 30% dwarf shrubs (Calluna vulgaris)	88-95% Sand, 2-9% Silt, 1- 2% Clay	rainfall exclusion for 4-6 weeks during spring and summer	None	2007- 2012	Kongstad <i>et al.</i> , 2012	
WB	-84.29/35.96	14.7	1440	1.1	343	Mixed composition of Quercus spp; Quercus prinus L., Quercus alba L., Quercus rubra L., Acer rubrum L., Acer saccharum, Liriodendron tulipifera L., Nyssa sylvatica Marsh. and Oxydendrum arboretum (L.)	28% Sand, 60% Silt, 12% Clay	-30% throughfall exclusion for the entire year	+33% rainfall for the entire year	1995- 2005	Hanson <i>et al.</i> , 2004	

Stubai	11.32/47.12	6.8	1382	1.7	970	C3 Grassland (Agrostis capillaris, Festuca rubra, Ranunculus montanus, Trifolium pratense, Trifolium repens)	42.2% Sand, 47% Silt, 10.8% Clay	rainfall exclusion for 8 weeks of summer rainfall	None	2009-2013	Fuchslueger <i>et al.</i> , 2014; Hasibeder <i>et al.</i> , 2015
--------	-------------	-----	------	-----	-----	--	----------------------------------	---	------	-----------	--

125

126 For all sites, aboveground NPP estimates (ANPP) were recorded for most of the experimental years derived by
 127 either biomass harvesting (grasslands) or biomass increase estimates derived from allometric relations and
 128 simultaneous observations of stem diameter, leaf area changes, plus litterfall (e.g., shrublands and forests). Leaf
 129 area index was quantified using the MODIS (MCD15A2H v006) estimate of the pixel containing each site.
 130 MODIS data were interpreted with caution as they are an indirect measurement, valid at typically larger scales,
 131 and prone to large uncertainties. For three sites, Konza, Puèchabon and WB, ET and gross primary productivity
 132 (GPP) were obtained at the half hourly scale by the Fluxnet2015 database and aggregated to the daily scale.

133 2.2 Participating models and simulation protocol

134 For all sites, we conducted simulations using ten terrestrial biosphere models: CABLE r54482.0 (Wang *et al.*,
 135 2011), DLEM v2.0 (Tian *et al.*, 2010), JULES v5.2 (Clark *et al.*, 2011), JSBACH v3.2 (Mauritsen *et al.*, 2019;
 136 Kaminski *et al.*, 2013), LPX v1.4 (Lienert and Joos, 2018), ORCHIDEE rev5150 (Krinner *et al.*, 2005),
 137 ORCHIDEE MICT rev5308 (Guimberteau *et al.*, 2018), ORCHIDEE CNP rev4520 (Goll *et al.*, 2017), T&C
 138 v1.0 (Fatichi, *et al.*, 2012; Paschalis *et al.*, 2017) and TECO v2.0 (Huang *et al.*, 2017). All models include a
 139 land surface scheme, a hydrological component, and a dynamic vegetation module. Soil moisture dynamics are
 140 simulated in multiple vertical layers by either solving the 1D Richards equation or simplified hydrological
 141 “bucket-type” models. Some models can simulate vegetation succession; however, this feature was disabled in
 142 the current study. Five models included nutrient dynamics. CABLE, DLEM, JSBACH and LPX simulated
 143 nitrogen and ORCHIDEE CNP nitrogen/phosphorus cycles. Hydrological and biogeochemical processes are
 144 simulated with a variable degree of complexity (for a detailed model description see the supplementary
 145 material of (Wu *et al.*, 2018)). As there is no commonly accepted way to simulate water limitation, each model
 146 has adopted significantly different approaches (Medlyn *et al.*, 2016b). Water stress in all models but T&C is a
 147 function of an average root zone soil moisture and in T&C, water stress is a function of the integrated root zone
 148 soil water potential. Specifically, models alter either photosynthetic rates (T&C, JULES, TECO), the maximum
 149 rate of carboxylation V_{cmax} (ORCHIDEE, ORC MICT, ORC CNP), stomatal conductance (JSBACH, DLEM),
 150 or a combination of all such parameters (CABLE), based on plant water availability. LPX uses a supply and
 151 demand driven approach to water limitation. If water demand exceeds supply, photosynthesis is downregulated

152 until they match. None of the models simulates plant hydraulics and thus xylem cavitation in response to water
153 stress.

154 For each site, we conducted a control simulation corresponding to the observed climate without manipulation,
155 and simulations representative of each rainfall manipulation experiment (rainfall exclusion and/or irrigation)
156 with the same timing and magnitude of water input as in the real experiment. For all experiments the common
157 data distributed to all modelling groups included hourly values of incoming shortwave and longwave radiation,
158 vapour pressure deficit, air temperature, wind speed, atmospheric pressure and ambient CO₂ concentration.
159 Model set-up was performed by each modelling group separately based on common information for each site
160 that included, apart from the meteorological input, species composition, vegetation cover, soil and root depth
161 and soil textural properties. Each modelling group translated independently this information into model specific
162 parameters. Dependent on the model, species composition and vegetation cover were used to either choose
163 between prescribed plant functional types (PFTs) or plant specific model parameters. Soil and root depth were
164 used by all modelling groups to set-up the simulation domain, and the vertical discretization of the simulation
165 was decided by each modelling group independently. Soil textural properties were used to select soil hydraulic
166 properties. All information concerning the simulation set-up of each model and the common site properties
167 provided to all modelling groups can be found at a free access data repository (see Data Sharing and
168 Accessibility statement). Reported model outputs included gross primary productivity, net primary productivity
169 and aboveground net primary productivity (GPP, NPP, ANPP), evapotranspiration (ET) and its partition in
170 evaporation (soil evaporation plus evaporation from interception) and transpiration respectively, soil moisture,
171 leaf area index (LAI) and biomass carbon pool (below and above ground) dynamics. Some models additionally
172 reported the water stress factor (β) used in the model. β is a model parameter that quantifies the effects of plant
173 physiological stress due to limitations in soil water availability. β is not identical between models and the
174 description of the β meaning for each model can be found at the supplementary material of Wu *et al.* (2018).
175 Initial conditions for all simulations were obtained after a spin-up period long enough to equilibrate the
176 biogeochemical cycles.

177 **2.3 Statistical Analyses**

178 ***Data-Model Comparison***

179 First, we compare the models' ability to accurately reproduce the relationship between ANPP and precipitation
180 (P) across sites (i.e. spatial dependence) and within each site (i.e. temporal dependence) at the annual scale. At
181 all sites, observations of ANPP were based on biomass estimates (e.g. using above ground biomass harvesting

182 for grasslands, and a carbon budget approach for forested sites combining litterfall observations with allometric
183 equation for aboveground biomass growth) rather than carbon fluxes, therefore discrepancy between observed
184 and modelled ANPP is expected (detailed bias quantification are reported in the Supplementary Material).

185 Model skill in reproducing the spatial dependence of ANPP to P was quantified as the root mean squared error
186 (RMSE) and the coefficient of determination (R^2) between the modelled and observed annual ANPP, averaged
187 over the entire period, across sites for the control case. Model performance in capturing the magnitude of
188 interannual variability of ANPP was assessed by comparing the standard deviation (σ) of annual ANPP
189 between models and observations for all sites. Model skill with respect to single-site interannual dependence of
190 ANPP to P was quantified using an estimate of the sensitivity of annual ANPP to annual P. Specifically, we
191 fitted a linear model $ANPP = a_0 + a_1P + a_2T$, where P is annual precipitation and T annual temperature. To
192 increase the sample size and robustness of the fit, precipitation from both the control and the rainfall
193 manipulation experiments were used. Additional covariates such as vapour pressure deficit and radiation could
194 not be added due to the small sample size, making the linear fit over constrained. Preliminary analyses (not
195 reported here) showed that P and T were the most important covariates. Model skill was evaluated by
196 estimating the differences between observed and simulated sensitivities of ANPP with respect to P (i.e. $a_1 =$
197 $\frac{\partial ANPP}{\partial P}$). Observation uncertainty of the sensitivity metric was quantified as the 90% confidence interval of the
198 linear model fit.

199 For the control simulations, modelled ET and GPP were compared with eddy covariance high frequency
200 observations from Walker Branch, Puèchabon and Konza. In these three locations, flux-tower data were
201 available in the proximity and with the same vegetation cover as the rainfall exclusion/addition experiment.
202 Comparison at the daily scale was performed by means of Taylor diagrams (Taylor, 2001). The magnitude and
203 seasonal pattern of the fluxes were also analysed (Supplementary material Figures S2-S4).

204 Responses due to rainfall manipulation were quantified at the annual scale using the response ratio for a
205 variable X (e.g. ANPP) defined as the ratio $RR = X_M^{(y)} / X_C^{(y)}$, where the subscript M stands for manipulation and
206 C for the control scenario. (y) indicates the annual scale. In this study, we focused on the simulated RRs of
207 ANPP and ecosystem water use efficiency (WUE) calculated at the annual scale as the ratio of annual gross
208 primary productivity (GPP) to annual actual evapotranspiration (ET). To quantify whether the simulated
209 response ratios have a statistically significant different mean value from the observations, a two-sample t-test
210 was performed for every model and the respective observed responses. For the two-sample t-test, the sample
211 size for each site is equal to the number of years in the observations and simulations. Response ratios were

212 assumed normally distributed and independent at the annual scale. The test's null hypothesis was that modelled
 213 and observed response ratios have the same mean. The analysis was also performed using the commonly used
 214 logarithm of RR yielding identical results, and thus not further shown here.

215 **Model agreement**

216 Model agreement across time scales was quantified by estimating the Pearson correlation coefficient (ρ)
 217 between all pairs of models for ET and GPP at the daily, monthly and annual scale. In the supporting material
 218 (Figure S7), the analysis is expanded for a wider range of scales by estimating the wavelet coherence between
 219 all pairs of models for ET and GPP.

220 To quantify agreement with respect to modelled changes in ANPP and WUE due to rainfall alterations, a two-
 221 sample t-test for the response ratios of both ANPP for all model pairs was performed and presented in the
 222 Supplementary material (Tables S2-S3).

223 To attribute the variability of ANPP to its causes we proceeded similarly to De Kauwe *et al.* (2017) who found
 224 that the annual ANPP could be approximated by the product

$$225 \quad ANPP = A_b \cdot CUE \cdot GPP_u \cdot \beta \cdot LAI_p \cdot LAI_r.$$

226 The term A_b is the aboveground fraction of carbon allocation, CUE is the carbon use efficiency, GPP_u is a
 227 potential (unstressed) rate of GPP per unit of leaf area, β is the annually averaged value of the water stress
 228 factor, LAI_p is the peak LAI during the year, and LAI_r is a proxy of the growing season length, defined as the
 229 integral of LAI during the year divided by LAI_p . Considering that water stress and LAI dynamics, determine
 230 most of the interannual variation of ANPP, assuming that A_b , CUE , and GPP_u vary less between treatments,
 231 then, the annual response ratio of ANPP can be estimated by the response ratios of β , LAI_p and LAI_r (e.g.

$$232 \quad \frac{ANPP_M^{(y)}}{ANPP_C^{(y)}} \approx \frac{\beta_M^{(y)}}{\beta_C^{(y)}} \cdot \frac{LAI_{pM}^{(y)}}{LAI_{pC}^{(y)}} \cdot \frac{LAI_{rM}^{(y)}}{LAI_{rC}^{(y)}},$$

where the subscript M stands for manipulation and C for the control scenario and

233 (y) indicates the annual scale). If the response ratios of β and LAI_p and LAI_r are independent at the annual
 234 scale, then

$$235 \quad \overline{\left(\frac{ANPP_M^{(y)}}{ANPP_C^{(y)}}\right)} \approx \overline{\left(\frac{\beta_M^{(y)}}{\beta_C^{(y)}}\right)} \cdot \overline{\left(\frac{LAI_{pM}^{(y)}}{LAI_{pC}^{(y)}}\right)} \cdot \overline{\left(\frac{LAI_{rM}^{(y)}}{LAI_{rC}^{(y)}}\right)},$$

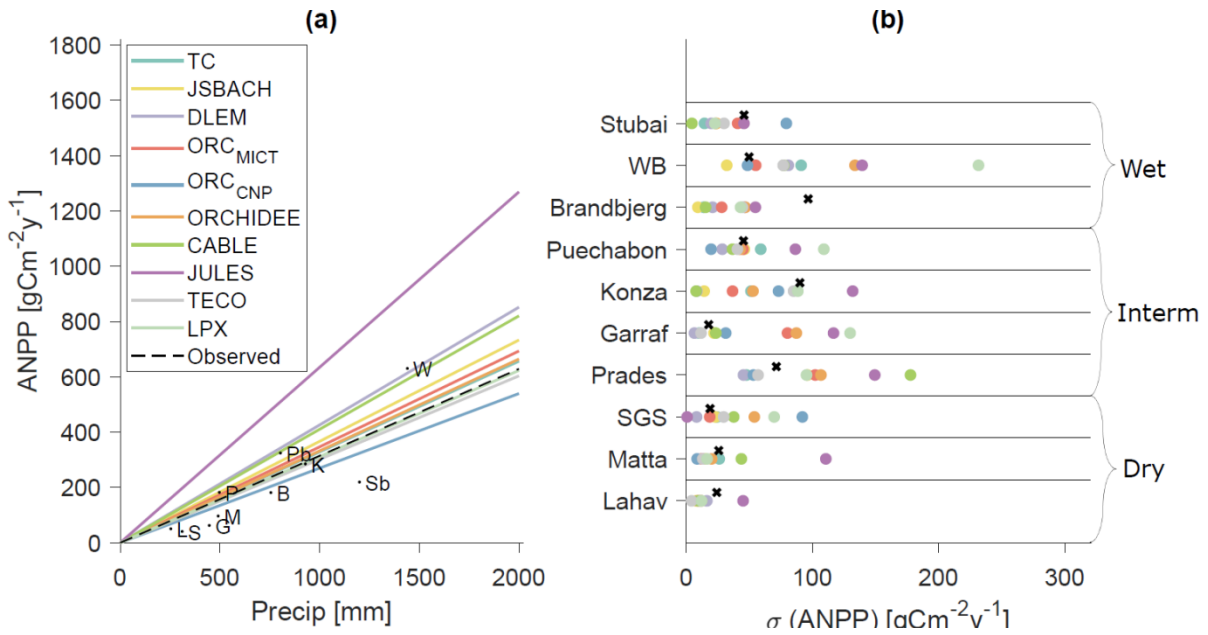
236 where overbars indicate average values for all years. This approximation is well supported by the results of our
 237 simulations (Supplementary material, Figure S6), even though data evidence suggests that CUE may change

238 significantly under changes in water stress (Rowland et al., 2014). Using this decomposition in the model
239 results, the average ANPP response ratio can be decomposed as the product of the average response ratios of
240 β, LAI_r, LAI_p . Based on these considerations, we can attribute the changes of the modelled ANPP among
241 models to differences in simulated water stress, LAI dynamics, and phenological changes. Since only six
242 (T&C, CABLE, JULES, TECO, DLEM, JSBACH) of the ten participating models reported the water stress β
243 factor, this analysis was performed using this subset of models. All statistical analyses were performed in
244 MATLAB 2019a.

245 **3 Results**

246 **3.1 Control Scenario**

247 Models captured the increasing trend of observed average ANPP to average P across sites (Figure 1a). The
248 RMSE between simulated and observed ANPP was in the range 23-354 g C m⁻² y⁻¹. Normalized RMSE of
249 ANPP was weakly but positively correlated ($R^2 = 0.36, p - value = 0.067$) with the RMSE of normalized
250 LAI (i.e. LAI divided by its maximum value). All models were positively biased. Positive biases can be
251 partially attributed to model shortcomings but can be also explained by experimental underestimations in
252 ANPP measurements (see Figure S1). Relative absolute biases (i.e. $|relBias| = \frac{|ANPP_{Mod} - ANPP_{obs}|}{ANPP_{obs}}$) are typically
253 larger at the driest sites ($\frac{\partial |relBias|}{\partial P} = -6.3 \cdot 10^{-4} \text{ mm}^{-1}$, estimated using ordinary least squares method).



254
255
256
257
258
259
260
261
262
Figure 1: (a) Dependence of mean annual ANPP to average annual precipitation during the study period. Letters indicate observed values (L: Lahav, M: Matta, S: SGS, P: Prades, G: Garraf, K: Konza, Pb: Puèchabon, B: Brandbjerg, W: WB, Sb: Stubai). Lines indicate, for each model, a least square fit of a linear relationship: $\text{ANPP}(P) = \alpha P$ between the modelled mean annual ANPP and mean annual Precipitation for all sites. (b) Standard deviation of modelled annual ANPP (circles) and observed annual ANPP (crosses) for all sites and models. Each model has a unique color indicated in the legend.

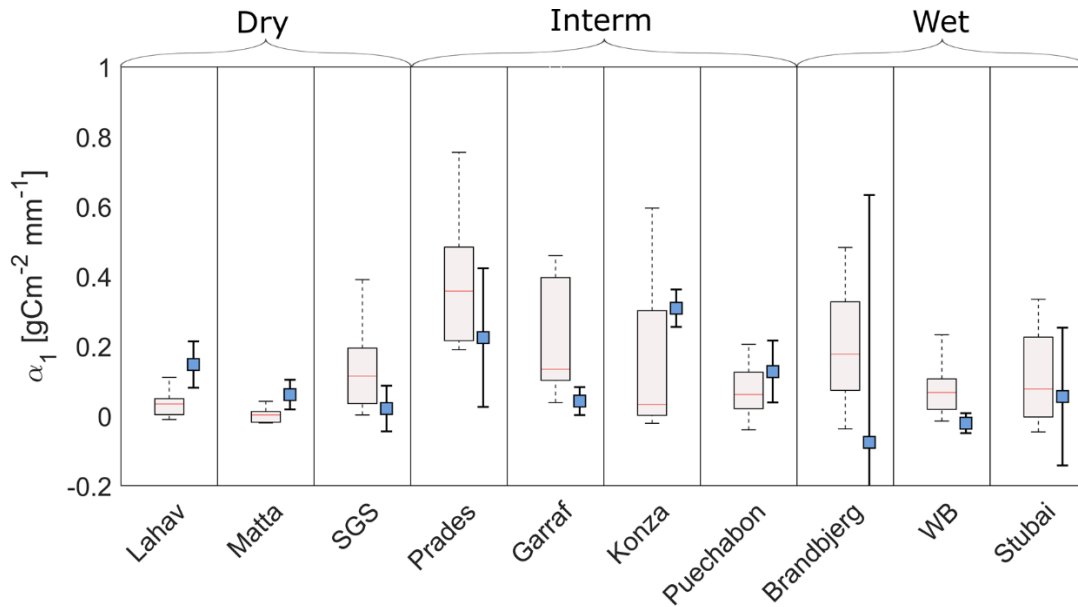
263
264
265
266
267
Table 2: Model skill across sites in terms of root mean square error (RMSE) for annual ANPP, normalized root mean square error (NRMSE) for annual ANPP, coefficient of determination for annual ANPP, average bias of ANPP, average bias of the standard deviation of annual ANPP, RMSE for daily LAI and RMSE for daily normalized LAI (i.e.

$$\frac{\text{LAI}}{\max(\text{LAI})} \cdot$$

Model	ANPP -			ANPP -		$\sigma(\text{ANPP})$	
	RMSE (gCm ⁻² y ⁻¹)	ANPP - Normalized RMSE [-]	ANPP - R ² [-]	Bias (gCm ⁻² y ⁻¹)	- Bias (gCm ⁻² y ⁻¹)	LAI - RMSE [m ² m ²]	LAI normalized RMSE [-]
TC	76.318	0.368	0.8295	30.7907	-13.5738	1.2399	0.2956

JSBACH	233.0982	1.1239	0.2379	79.3713	-19.6096	1.2972	0.4276
DLEM	202.8963	0.9783	0.7732	96.935	-23.7873	1.2038	0.356
ORC MICT	121.7962	0.5872	0.6131	51.5792	-5.7495	1.1895	0.3966
ORC CNP	210.5444	1.0151	0.041	15.0756	-1.0366	1.1451	0.4198
ORCHIDEE	113.8664	0.549	0.6489	44.8288	9.3944	1.2675	0.3505
CABLE	215.6812	1.0399	0.4728	115.9473	-5.1951	2.147	0.3437
JULES	354.0429	1.707	0.4399	278.4353	39.4962	1.4164	0.449
TECO	23.3013	0.1123	0.982	5.3858	-9.3174	1.1347	0.3462
LPX	113.6602	0.548	0.5956	36.4618	33.2501	1.3886	0.4317

268



269

270

271

272

273

274

275

276

Figure 2: Simulated and observed sensitivity of annual ANPP to annual precipitation ($\alpha_1 = \frac{\partial \text{ANPP}}{\partial P}$). For each site, boxplots indicate the distribution of the simulated sensitivity of ANPP to precipitation by all models. Error bars show the sensitivity of observed ANPP to precipitation (blue squares) and the corresponding 90% confidence intervals (bar length) of the fit of the linear model. Crosses indicate the sites for which the mean value of the distribution of simulated sensitivities is not statistically different from the observed with 90% confidence. Sites are ranked from left to right in order of ascending wetness.

277

278

Both models and observations support a larger sensitivity of annual ANPP to interannual variation in precipitation at sites with intermediate wetness conditions (e.g. Garraf, Prades, Puechabon, Konza; Figure 2).

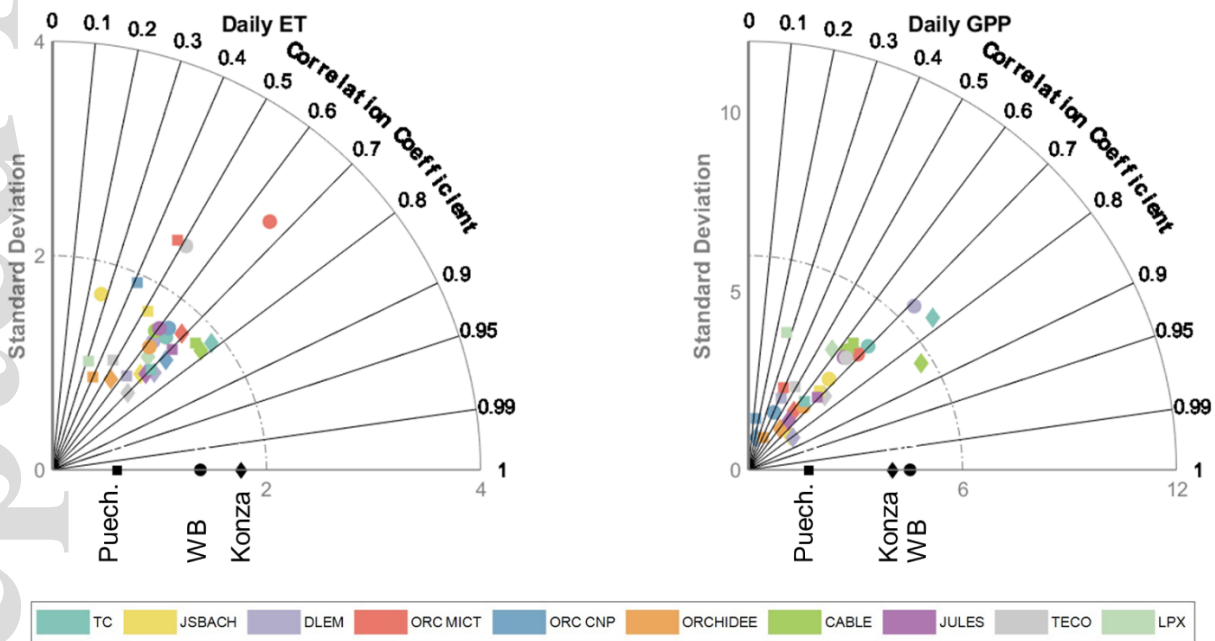
279 Specifically, in sites with a wetness index $WI < 0.4$ models(observations) have mean sensitivity $\overline{a_1} = 0.058$
280 $(0.076) \text{ gCm}^{-2}\text{mm}^{-1}$, in sites with $0.4 \leq WI < 1$, $\overline{a_1} = 0.22(0.18) \text{ gCm}^{-2}\text{mm}^{-1}$ and in sites with $WI > 1$,
281 $\overline{a_1} = 0.13(-0.013) \text{ gCm}^{-2}\text{mm}^{-1}$. At the most arid sites, annual precipitation explains a large fraction of the
282 observed and modelled variability of annual ANPP, but the sites are not highly productive (i.e. Absolute
283 productivity values are low; Figure 1), yielding a low average sensitivity a_1 . At the opposite end, mesic sites
284 have higher productivity, but they are not water limited during the observation period, resulting also in a low
285 modelled sensitivity $\overline{a_1}$. Modelled sensitivity uncertainty was largest for intermediate precipitation regimes due
286 to a larger model disagreement for those sites. For sites with a $WI < 0.4$, the average uncertainty, quantified
287 here as the standard deviation between models of modelled a_1 was $\sigma_{a_1|dry} = 0.08 \text{ gCm}^{-2}\text{mm}^{-1}$, for
288 intermediate sites $\sigma_{a_1|inter} = 0.24 \text{ gCm}^{-2}\text{mm}^{-1}$ and for wet sites $\sigma_{a_1|wet} = 0.14 \text{ gCm}^{-2}\text{mm}^{-1}$.

289 On average, the modelled sensitivity of ANPP to precipitation within sites was lower ($\sim 0.15 \text{ gCm}^{-2}\text{mm}^{-1}$)
290 than ($\sim 0.37 \text{ gCm}^{-2}\text{mm}^{-1}$; estimated as the average slope of the linear models reported in Figure 1a) between
291 sites. However, the uncertainty of the estimated temporal sensitivity from observations, as quantified by the
292 90% confidence limits of the linear model, is very high in most sites ($0.29 \text{ gCm}^{-2}\text{mm}^{-1}$, averaged across all
293 sites) and comparable to the uncertainty between models ($\overline{\sigma_{a_1}} = \sigma'_{a_1} = 0.14 \text{ gCm}^{-2}\text{mm}^{-1}$, averaged across all
294 sites). A large uncertainty is related to either a small sample size, or low skill of the linear model. As a result, it
295 is not possible to robustly quantify whether the modelled temporal sensitivities are statistically different from
296 the observed ones, but overall only six out of ten sites had mean modelled that were not non-statistically
297 scientifically different than the one observed (Figure 2).

298 Simulated daily ET for the control simulations was substantially different regarding its day-to-day variability
299 from measured ET at all three eddy sites (Konza, Puèchabon, WB). Correlation coefficients were in the range
300 $0.27-0.78$ with an average value between all models and sites of $\sim 0.60 \pm 0.13$ (mean \pm standard deviation)
301 (Figure 3). Simulated variability of ET, expressed in terms of standard deviation at the daily scale, deviated
302 substantially from the measured variability of ET. In particular, simulated variability from most models was
303 lower than observed at Konza (observed $\sigma_{ET} = 1.76 \text{ mm d}^{-1}$, modelled $\sigma_{ET} = 1.40 \pm 0.3 \text{ mm d}^{-1}$), and
304 higher than observed at Puèchabon (observed $\sigma_{ET} = 0.61 \text{ mm d}^{-1}$, modelled $\sigma_{ET} = 1.86 \pm 0.50 \text{ mm d}^{-1}$). For
305 WB, the modelled ET variability was higher than observed, and inter-model agreement was low (observed σ_{ET}
306 $= 1.39 \text{ mm d}^{-1}$, modelled $\sigma_{ET} = 1.51 \pm 0.45 \text{ mm d}^{-1}$). Seasonality of ET was well reproduced by all models
307 (Figure S2), partially explaining the high correlation coefficients (Figure 3). One pronounced exception is in

308 Puèchabon, where the observed late summer reduction of ET and increase in early fall was reproduced only by
 309 a small subset of models (Figure S2).

310 Simulated daily GPP had a correlation ($\sim 0.59 \pm 0.17$) with observed daily GPP for all models (Figure 3). A
 311 large fraction of the GPP correlation can be attributed to seasonality. However, the modelled variability was
 312 significantly different from the observed for all sites. Most models underestimated the daily variation of GPP at
 313 Konza (observed $\sigma_{GPP} = 4.04 \text{ gCm}^{-2}\text{d}^{-1}$, modelled $\sigma_{GPP} = 2.87 \pm 1.88 \text{ gCm}^{-2}\text{d}^{-1}$) and WB (observed
 314 $\sigma_{GPP} = 4.53 \text{ gCm}^{-2}\text{d}^{-1}$, modelled $\sigma_{GPP} = 4.01 \pm 1.26 \text{ gCm}^{-2}\text{d}^{-1}$) and overestimated the variability of
 315 daily GPP at Puèchabon (observed $\sigma_{GPP} = 1.68 \text{ gCm}^{-2}\text{d}^{-1}$, modelled $\sigma_{GPP} = 2.67 \pm 1.01 \text{ gCm}^{-2}\text{d}^{-1}$)
 316 (Figure 3). Large model differences between observed and simulated GPP can be partially attributed to an
 317 incorrect representation of the magnitude of LAI. There is, indeed, a large disagreement between the modelled
 318 LAI across models (Figure 4). Modelled LAI is also significantly different than observed, even though LAI
 319 derived via remote sensing is also uncertain (Fang *et al.*, 2013).



320

321 *Figure 3: Taylor Diagrams for daily evapotranspiration (ET) and gross primary productivity*
 322 *(GPP) for all models and all sites with available flux tower data. Models are indicated with*
 323 *different colors according to the legend. Each site has a different marker (diamond for*
 324 *Konza, circle for WB and square for Puèchabon). The ideal model (i.e. reproducing precisely*
 325 *the data) would lie on the black markers, each corresponding to different sites.*

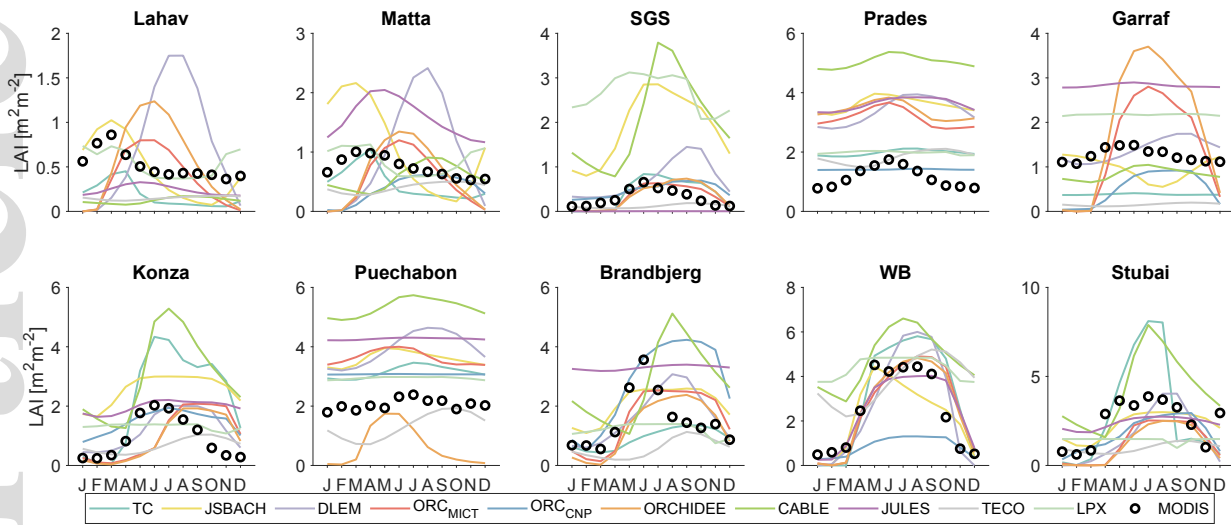
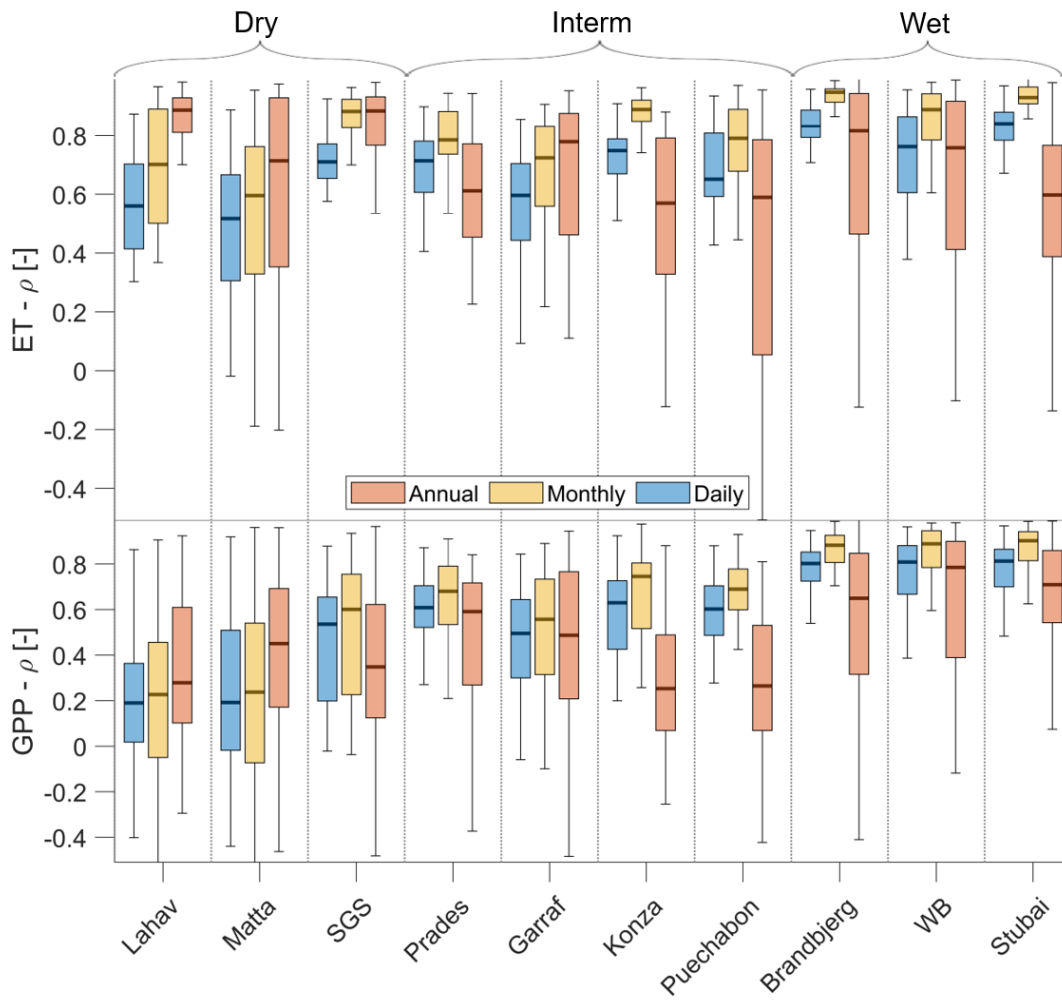


Figure 4: Simulated average monthly LAI by all models for all sites for the control case simulation. Dots indicate the long-term monthly LAI averages of the nearest MODIS pixel in the area.

Model agreement in terms of ET and GPP varies also with time scale (Figure 5). In the driest sites (e.g. Lahav, Matta, SGS; $WI < 0.4$), models agree mostly with each other on the interannual variability of ET (average corr. coef. ρ for ET at the annual (y) scale $\rho_{ET|dry}^y = 0.75$; for GPP $\rho_{GPP|dry}^y = 0.35$). This is expected since at those sites annual ET almost equals the total amount of rainfall. However, a significant model disagreement occurs at the daily (d) scale ($\rho_{ET|dry}^d = 0.58$, $\rho_{GPP|dry}^d = 0.30$). The opposite picture occurs in mesic sites ($WI > 1$), where models agree better at the daily time scale for ET ($\rho_{ET|wet}^d = 0.79$), but their agreement is significantly lower at the annual scale ($\rho_{ET|wet}^y = 0.61$). A similar pattern is also valid for GPP ($\rho_{GPP|wet}^d = 0.77$; $\rho_{GPP|wet}^y = 0.60$) (Figure 5).

Model agreement with regards to the dependence of the water stress factor β on root averaged soil moisture $\theta(Z_r)$ is also low (Figure 6). On average model agreement was highest for sites with a large percentage of sand (Brandbjerg 88-95% sand, Prades 48% sand) and lowest in sites with soils rich in more fine material (e.g. Lahav 22% sand, Matta 19% sand, SGS 14% sand, Konza 10% sand).



343

344

345

346

Figure 5: Boxplots of Pearson correlation coefficients between simulated ET and GPP for all pairs of models for three time scales (daily, monthly, and annual) for all ten sites. Scales are indicated with different colors according to the legend.

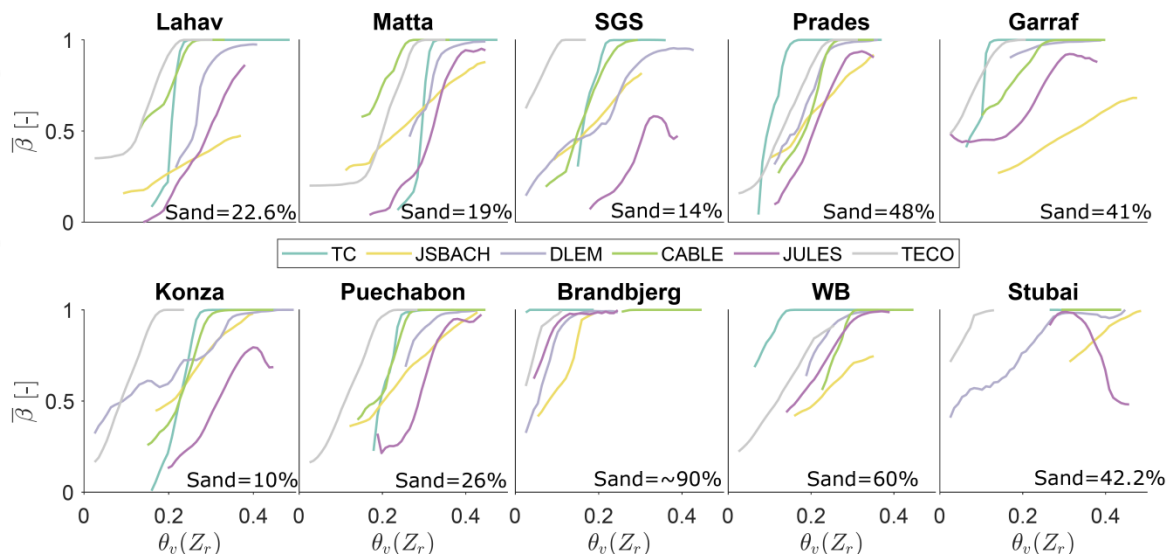


Figure 6: Average simulated water stress factor β as a function of root zone averaged soil moisture. For all sites and models $\bar{\beta}$ corresponds to the simulated average value of β at the daily scale for overlapping bins with soil moisture width 0.05.

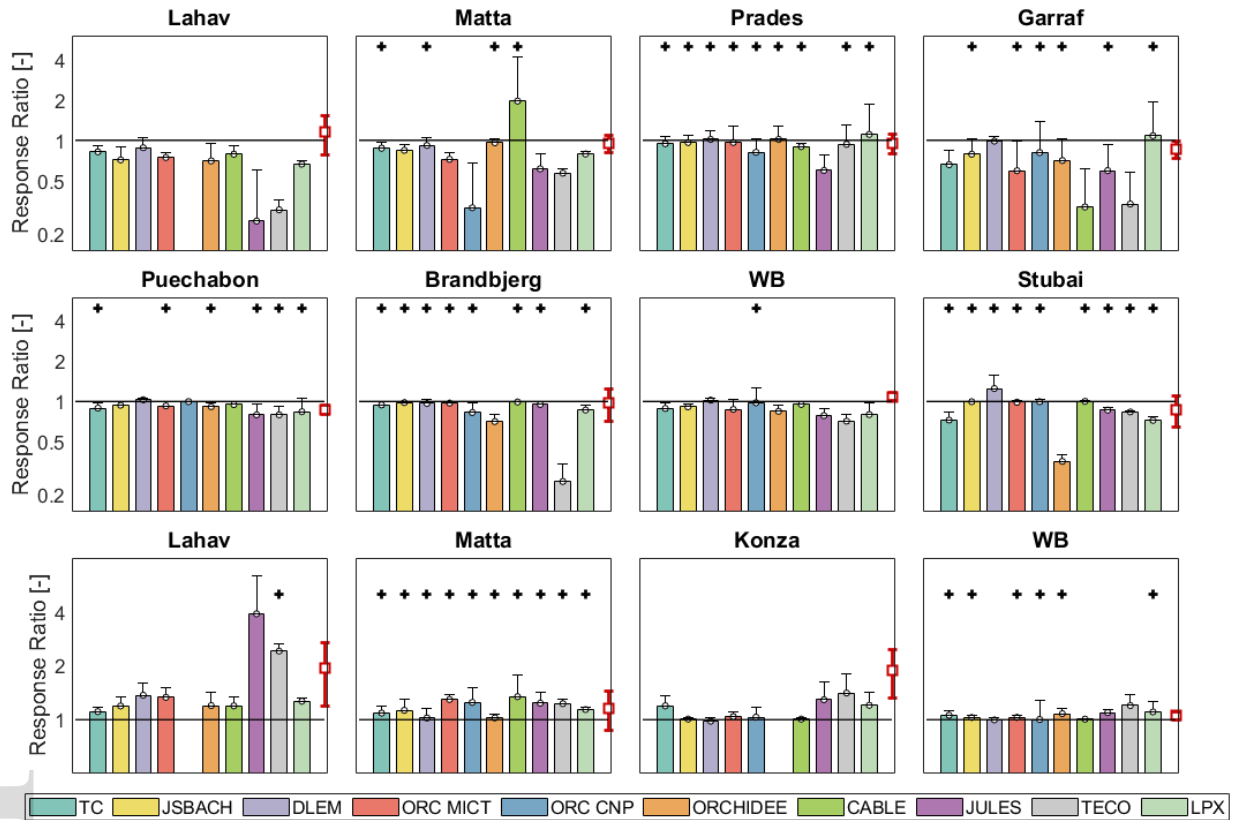
3.2 Manipulation Experiments

Models were tested for their skill at reproducing changes in ANPP due to rainfall manipulations (Figure 6). Most models (75% for model-site-treatment combinations) correctly predicted the sign of the change in ANPP. However only 54% of the models for the drought treatment (10 models \times 8 sites) and 43% for the irrigation treatment (10 models \times 4 sites) have a mean response that is statistically similar in magnitude with the observed, highlighting a better model performance for rainfall exclusion than addition. The worst performance of the models was obtained for both the drought and irrigation experiments in Lahav and in the irrigation experiment in Konza where almost no model was able to capture the correct magnitude of the response ratio.

Even though observed ANPP estimated from biomass should be close to modelled ANPP (Figure S1) several uncertainties related to observations, such as the choice of biomass harvest date, the use of specific allometric equations, and specific local conditions could affect our results. For instance, the observed response to irrigation in Lahav and Matta is considerably different despite the two sites having similar vegetation and climate. Those differences are either due to measurement uncertainties, or due the large effect of some local properties (e.g. soil composition, nutrient availability (Golodets *et al.*, 2013, 2015)) causing significant changes in the ecosystem dynamics. Overall, the magnitude of responses is similar amongst models except CABLE, JULES and TECO, which show a larger sensitivity of ANPP to rainfall manipulation. Modelled interannual

367 variability of the responses was in most cases similar in magnitude to the observed for the rainfall exclusion
 368 experiments, and lower for the irrigation experiments (for the drought experiments: average modelled standard
 369 deviation of the response ratios was $\sigma_{RD}^m = 0.18$; and observed $\sigma_{RD}^o = 0.178$. For irrigation experiments
 370 modelled standard deviation was $\sigma_{RI}^m = 0.25$; and observed $\sigma_{RI}^o = 0.42$). Outliers with regards to both the
 371 magnitude and the interannual variability of response ratios occurred for the most water-limited sites.

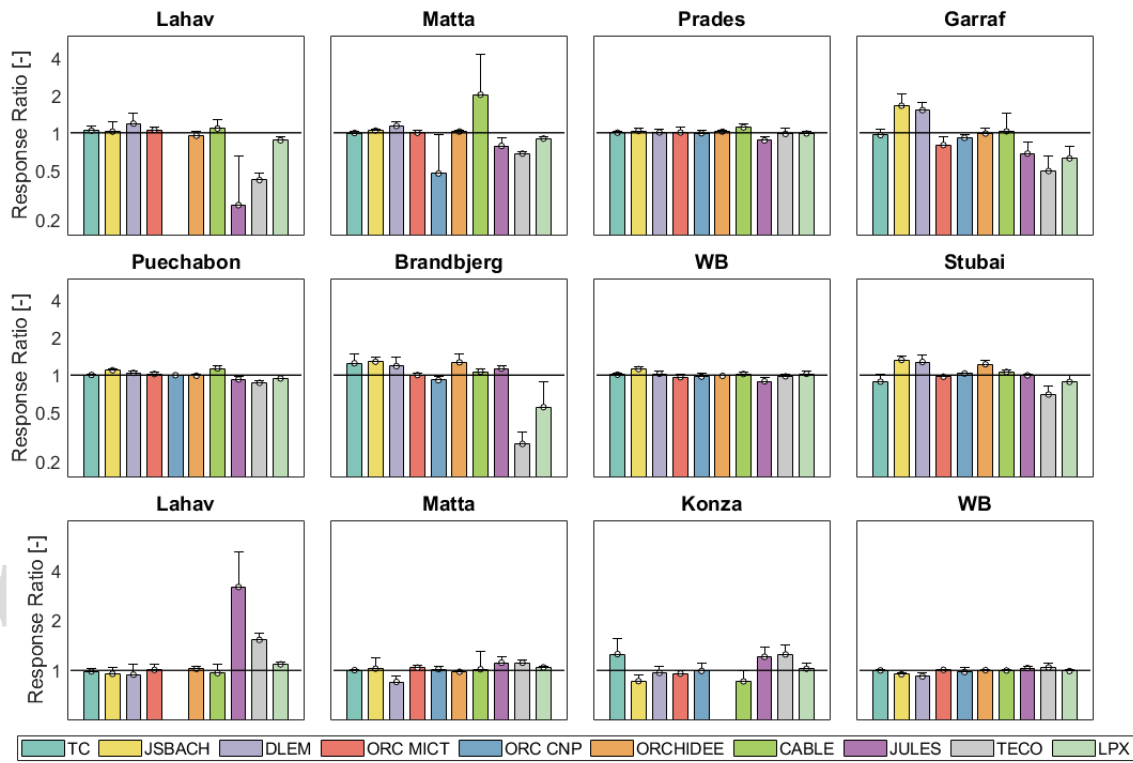
372



373

374 *Figure 7: Simulated and observed response ratios of annual ANPP due to rainfall exclusion*
 375 *(rows 1 and 2) and addition (irrigation) (row 3). Different models are presented with*
 376 *different colors according to the legend. Error bars represent the standard deviation for all*
 377 *years of treatment. Red error bars represent measured response ratios. Black crosses*
 378 *indicate models where the null hypothesis of the same mean between simulated and observed*
 379 *response ratios is not rejected based on a two sample t-test. Missing bars relate to spurious*
 380 *model output due to loss of vegetation survival.*

381 Besides carbon assimilation, changes in rainfall can simultaneously modify ET and thus the land surface
 382 energy balance. The coupling between ET and GPP depends heavily on the parametrizations of water stress
 383 and how this affects stomatal conductance and the reduction of photosynthesis. It further depends on vegetation
 384 dynamics such as a shift of carbon allocation from leaves to roots or leaf shedding due to water stress. To
 385 quantify the responses of the ET and GPP coupling, we compute the relative changes of water use efficiency
 386 (WUE) for the various cases (Figure 8). Most models predict relatively small changes in WUE (i.e. $R \sim 1$) for
 387 both drought ($R_D^m = 0.98$) and irrigation ($R_I^m = 1.08$) treatments, indicating a change of comparable
 388 magnitudes for both ET and GPP. CABLE, JULES and TECO occasionally simulate larger changes, in both
 389 positive and negative directions, in WUE for the most water limited sites. This larger change can be attributed
 390 to a more sensitive response of GPP to water stress than ET.



391

392

393

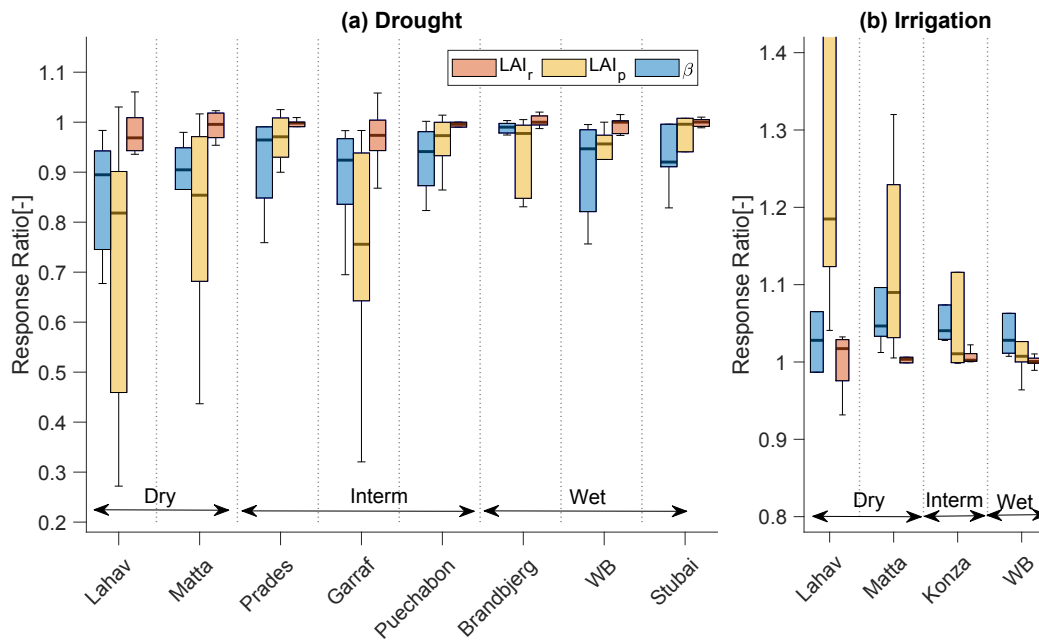
Figure 8: Simulated response ratios of water use efficiency during treatment period per year due to rainfall exclusion (rows 1 and 2) and addition (irrigation) (row 3). Different models

394 are presented with different colors according to the legend. Error bars represent the
395 standard deviation for all years of treatment.

396

397 3.3 Response attribution

398 We partitioned the total response ratio of ANPP into relative changes of (a) the β stress factor; (b) peak LAI (
399 LAI_p); and (c) the length of the growing season approximated by LAI_r (Figure 9). Changes in simulated ANPP
400 following rainfall manipulation can be almost exclusively attributed to changes in β and LAI_p . The response
401 ratio of LAI_r was always close to unity ($R_{LAI_r} = 0.98 \pm 0.058$ (mean \pm standard deviation) for the drought
402 treatment and $R_{LAI_r} = 1.01 \pm 0.029$ for the irrigation treatment) contributing insignificantly to the response
403 ratio of ANPP. Thus, no model predicted substantial changes in the length of the growing season. A reduction
404 or enhancement of β for the drought and irrigation experiments explained the largest fraction of ANPP
405 responses at wet sites, but the uncertainty of the relative strengths of changes in β and LAI_p was high (Drought
406 treatment for sites with $WI > 1$, $R_\beta = 0.95 \pm 0.08$, $R_{LAI_p} = 0.91 \pm 0.18$; Irrigation treatment for sites with
407 $WI > 1$, $R_\beta = 1.05 \pm 0.06$, $R_{LAI_p} = 1.02 \pm 0.02$). For the driest sites both LAI_p and β explained a large fraction
408 of the total response for the drought treatment, whereas LAI_p was the dominant and simultaneously the most
409 uncertain factor for the irrigation treatment (Drought treatment for sites with $WI < 0.4$, $R_\beta = 0.87 \pm 0.10$,
410 $R_{LAI_p} = 0.77 \pm 0.24$; Irrigation treatment for dry sites with $WI < 0.4$, $R_\beta = 1.06 \pm 0.10$, $R_{LAI_p} = 1.49 \pm 0.86$).
411 Differences in the simulated responses of both β and LAI_p amongst models was high as indicated by the
412 standard deviations above. At the sites where rainfall exclusion was applied only in part of the year (Garraf,
413 Brandbjerg) the response ratio of LAI_p was larger than the reduction of β ($R_\beta = 0.93 \pm 0.09$, R_{LAI_p}
414 $= 0.78 \pm 0.27$), but given the large variability amongst models, it is not possible to conclude if this is a true
415 signal. The variability was higher for the most water stressed sites, primarily because for those sites model
416 disagreement on the estimated response ratio of ANPP was also the highest.



418

419

Figure 9: Boxplots of the response ratios of the change of β , LAI_p and LAI_r as simulated by (T&C, JSBACH, DLEM, CABLE, JULES and TECO) for the drought experiments (a) and the irrigation experiments (b).

420

421

422 4 Discussion

423

Multi-site and local sensitivities to rainfall and the role of temporal scales

424 Most models overestimated the relationship between mean annual precipitation and average annual ANPP
 425 observed across sites, but managed to capture well the overall trend, despite large site differences in terms of
 426 vegetation coverage and overall climatic regime (Figure 1). This result confirms that terrestrial biosphere
 427 models can capture spatial gradients of vegetation productivity relatively well (e.g. Wu *et al.*, 2018).
 428 Reproducing local (single-site) response of ANPP to interannual precipitation variability has been generally
 429 found to be more challenging (Fatichi and Ivanov, 2014). In fact, previous intercomparison studies have found
 430 that models have significant biases at various time scales, from subdaily (Matheny *et al.*, 2014) to decadal
 431 (Dietze *et al.*, 2011). Dietze *et al.*, (2011) found model errors to be largest at the annual scale. In agreement
 432 with such a result in our experiment, models differed greatly in their simulated sensitivity of local scale
 433 productivity to annual precipitation but were able to reproduce the previously reported stronger spatial than

434 temporal sensitivity of productivity to rainfall. A large model disagreement with regards to the magnitude of
435 the interannual variability of ANPP also confirms the previously found difficulties of models to properly
436 capture carbon dynamics at the annual scale (e.g. Dietze *et al.*, 2011, Paschalis *et al.*, 2015). Despite large
437 model disagreement we found that the within site sensitivity of ANPP to precipitation is lower than across site
438 sensitivity of ANPP to average precipitation, in agreement with a number of previous observational (Goward
439 and Prince, 1995; Knapp and Smith, 2001; Huxman *et al.*, 2004) and modelling results (Fatichi and Ivanov,
440 2014; Wu *et al.*, 2018).

441 One of the main reasons for model disagreement originates from the differences in parametrization in schemes
442 representing water limitation effects on water and carbon fluxes (e.g. Trugman *et al.*, 2018), summarized here
443 by the water stress parameter β (Figure 6). Those parametrizations influence ecosystem dynamics at a wide
444 range of temporal scales, complicating assessment of their skill. For instance, at shorter time scales (e.g. daily),
445 in ecosystems with no water limitation, where temperature and radiation are the dominant controls for ET and
446 GPP (Paschalis *et al.*, 2015), models had a high agreement (Figure 5), in terms of correlation. This highlights
447 that parametrizations that impact the temporal changes of ET and GPP should be relatively consistent among
448 models, at least during wet conditions (Ukkola *et al.*, 2016). Even though correlation between models was
449 high, large variability between models with regards to the actual magnitude of the fluxes was pronounced
450 (Figure S2-S4), primarily for carbon fluxes (e.g. GPP). This indicates that a “scaling” factor affecting GPP is
451 significantly different amongst models. For our experiments, LAI could be this explanatory “scaling” factor
452 (Figure 4), as models greatly differed regarding the seasonality and magnitude of LAI.

453 Significant changes emerge under drought, when water stress parametrizations influence the simulation of
454 water and carbon fluxes. Different water stress parametrizations alter the water/carbon dynamics at different
455 scales. In severely water-limited systems ($WI < 0.4$), model results diverge in terms of GPP and ET at short
456 temporal scales (e.g. daily - Figure 5). Thus, parametrizations of how water stress impacts processes operating
457 at daily and sub daily time scales are crucial, and highly diverging amongst models. Such parametrizations
458 include stomatal regulations and downregulation of photosynthesis during drought. In general, plant hydraulic
459 dynamics will also operate at these temporal scales, but none of the participating models simulated such
460 processes in detail. In severely water limited ecosystems the amount of annual precipitation imposes a strong
461 constraint on evapotranspiration (i.e. $ET \cong P$), leading to overall good agreement between models for annual
462 ET. However, this agreement is not true for transpiration alone (Figure S8), highlighting the major importance
463 of how stomatal limitations are implemented in models. Physical constraints for productivity are not as strong,
464 and thus models have large disagreement with respect to GPP even at annual scales.

465 In intermediate wetness sites ($0.4 \leq WI < 1$), in our simulations, models disagree at intermediate scales
466 (weeks-months) in terms of GPP (consistent with the wavelet coherence analysis presented at Figure S7). As
467 mentioned before, at short (daily) temporal scales, temperature and radiation mostly determine water and
468 carbon fluxes, when water is not a strong limiting factor, and due to the similar parametrizations among models
469 (Wu *et al.*, 2018), we detect a substantial convergence in GPP. However, since such controls “fade” with
470 increasing temporal scales, the effects of features linked to soil moisture dynamics, such as the soil moisture
471 retention after a rainfall event, can manifest at longer temporal scales (Paschalis *et al.*, 2015). Those dynamics
472 can be influenced by factors including both biotic and abiotic factors such as the parametrizations of soil
473 properties that determine the temporal dynamics of soil moisture and the vertical distribution of root biomass,
474 affecting how plants withdraw water from the soil. In fact, models were found to strongly disagree on how
475 plants are affected by soil moisture (biotic factor – Figure 6) and on the soils’ water holding capacity, as
476 indicated by the range of accessible values of soil moisture (abiotic factor – Figure 6).

477 At the wettest sites ($WI > 1$), strong model disagreement in terms of both water and carbon fluxes occurs at
478 annual scales. A key factor for model disagreement for those sites is LAI (Figure 4). Model disagreement in
479 LAI is a composite effect of the water stress impacts to LAI development and the overall model disagreement
480 in leaf phenology and carbon allocation rules (Figure 4; Richardson *et al.*, 2012).

481 All those behaviours highlight further the need to correctly capture water/carbon dynamics at multiple time
482 scales, from the scale of the individual rain pulse (Huxman *et al.*, 2004a) up to interannual scales where
483 drought legacies can have an important effect (Anderegg *et al.*, 2015). The need to understand in detail multi-
484 scale dynamics linked to water stress and soil moisture dynamics is also exacerbated by the fact that model
485 disagreement in terms of the sensitivity of ANPP to annual rainfall is highest for sites with intermediate
486 wetness ($0.4 \leq WI < 1$). Those regions experience moderate water limitations, and the impact of water
487 limitation to fast acting processes (changes in e.g. stomatal conductance, photosynthesis) can accumulate and
488 impact longer time scales through slow acting processes (e.g. changes in LAI). Additionally, areas with
489 intermediate wetness are expected to operate close to soil moisture thresholds inducing plant water stress.
490 Sensitivity of the responses of ANPP to precipitation in those sites is concurrently the highest and most
491 uncertain (Figure 2). This can have a large impact on our ability to model the fate of terrestrial CO_2 , given that
492 those areas are amongst the largest contributors to the interannual dynamics of the growth rate of CO_2 (Poulter
493 *et al.*, 2014; Ahlström *et al.*, 2015). Understanding such dynamics across scales requires high quality and high
494 frequency long-term measurements, not only for CO_2 and water fluxes but also soil moisture dynamics (Vicca

495 *et al.*, 2012). Annual ANPP values alone are limiting our inference capabilities and even 10-20 years of annual
496 ANPP data were not long enough to obtain a precise estimate of the sensitivity of ANPP to precipitation.

497 Uncertainties arise from the relatively short span of the record, but also due to the lack of data describing short-
498 scale dynamics of carbon assimilation and growth in manipulation experiments. Annual precipitation has been
499 found to be a relatively weak descriptor of the interannual variability of water and carbon fluxes in many
500 locations worldwide (Fatichi and Ivanov, 2014). A better descriptor would be the time duration during a year
501 when favourable meteorological conditions for photosynthesis occur under well-watered conditions (Fatichi
502 and Ivanov, 2014; Zscheischler *et al.*, 2016a). As a result, a few bursts of positive extremes in terms of
503 productivity can strongly modify the annual budget and long-term dynamics (Zscheischler, *et al.*, 2014a).
504 Therefore, to quantify the interannual dynamics of vegetation productivity, detailed knowledge of water/carbon
505 fluxes, meteorology, soil moisture and plant water status at fine temporal scales would be essential. In fact,
506 previous research at the PHACE experiment, one of the few facilities that combined such high frequency
507 measurement clearly identified the problems models have in reproducing sub-annual dynamics (De Kauwe *et*
508 *al.*, 2017). Given the present limited availability of such data, new ways of combining existing data (e.g.,
509 combining different data-streams representing short and long-term-dynamics in multiple locations, such as
510 Fluxnet sites for water and carbon fluxes at high frequencies, sites equipped with phonecams for high
511 frequency phenology monitoring, soil moisture networks (e.g. COSMOS, the International Soil Moisture
512 Network, the Long Term Ecological Research Network etc.), open access data archiving with common data
513 formats to facilitate data exchange between research groups and the use of proxy data to extend the length of
514 the time series (e.g., tree rings) are necessary to better inform models (Pappas *et al.*, 2017; Babst *et al.*, 2018).

515 ***Response to manipulation experiments***

516 The modelled sensitivities of vegetation dynamics to changes in rainfall are highly uncertain. On average, most
517 models captured better the observed responses of vegetation to rainfall exclusion than addition (Figure 7). That
518 behaviour can be associated with low skill in reproducing the asymmetric response of productivity to
519 precipitation (Wu *et al.*, 2018), failing to capture the correct pattern of the productivity saturation effect
520 associated with rainfall increase.

521 Even though, multiple models generated close vegetation productivity responses in the rainfall exclusion
522 experiments, the underlying reasons are very different and at the same time highly uncertain (Figure 9). In the
523 more water-limited ecosystems, both changes in LAI magnitude and the level of plan water limitation
524 determine productivity responses. Variability of the relative strength of β and LAI_p between models is large.

525 Variability concerning LAI_p is larger than β , which can be explained by the fact that LAI_p integrates the model
526 differences related to LAI phenology, carbon allocation rules, and reductions in photosynthetic rates due to soil
527 moisture limitations. Pinpointing which model best captures the relative strengths of changes in β and LAI_p
528 would require simultaneous high frequency data, including soil moisture, regular measurements of stomatal
529 conductance and leaf water potentials, high frequency photosynthetic rates, and regular LAI estimates. At more
530 mesic sites, physiological effects of water stress (through β) are the main reason for productivity responses.
531 The reason is that in such sites, induced water stress is mild. Productivity will be reduced during the imposed
532 water stress due to rainfall exclusion, but this small increase in water stress cannot cause large changes in
533 vegetation structure (Estiarte *et al.*, 2016), or LAI .

534 Disagreement in irrigation experiments is primarily related to leaf area dynamics. The reason can be that in the
535 simulations where water stress was relieved, model disagreement originates primarily from the leaf area
536 dynamics simulated for the unstressed conditions. Those dynamics are related to the choice of carbon
537 allocation and leaf phenology algorithms. Pronounced model differences related to those dynamics can be
538 shown via the magnitude and seasonal patterns of LAI (Figure 4) as simulated by all models. Both the
539 allocation and the phenology algorithms affect the dynamics of LAI . In our simulations (Figure 4) the range in
540 modelled LAI is large and comparable with that reported by previous studies (Walker *et al.*, 2014; De Kauwe
541 *et al.*, 2017). Parametrizations of carbon allocation and are also limited by generic plant functional types
542 (PFTs) used by most models. Such a choice is generally very restrictive and cannot capture the natural
543 variability of plant traits, which is relevant at the local scale.

544 In our analysis changes in growing season length were not evident and did not influence our results. This is not
545 surprising, as all rainfall manipulation experiments decreased or increased the available water to the ecosystem,
546 without altering its “pulse” structure, including the frequency of rainfall occurrence, and the time of storm
547 arrival (Ross *et al.*, 2012). As vegetation phenology in water limited ecosystem is very sensitive to the pulse
548 structure dynamics of rainfall (Heisler-While *et al.*, 2009), evaluating in future experiments, whether models
549 can properly capture the responses of vegetation to rainfall pulses in terms of productivity and drought
550 deciduousness is very important. Changes in rainfall pulses will also strongly impact soil respiration dynamics,
551 that will contribute significantly to the total carbon balance (Unger *et al.*, 2010; Jarvis *et al.*, 2007).

552 ***Outlook for model developments and observations***

553 Our results highlight the need for a coordinated effort of new model development and data collection that could
554 enable validations that are much more detailed than currently achievable here. Model discrepancies in the

555 present study were attributed to the β stress factor, and long-term leaf area dynamics. The models used in this
556 study implemented simple conceptual, yet vastly different (Wu *et al.*, 2018) parametrizations of the effects of
557 water limitation, neglecting plant hydraulics and thus impacts on the water transport system (xylem cavitation)
558 that can lead to hydraulic failure or/and carbon starvation (McDowell, 2011; McDowell *et al.*, 2013; Bonan *et*
559 *al.*, 2014; Xu *et al.*, 2016). This could be an important limitation. However, tree mortality is not a prominent
560 feature of the manipulation experiments considered here and while it has attracted a lot of attention, models
561 first need to better simulate mild to severe water stress before considering vegetation death. For instance,
562 differences associated with the β factor are not only related to plant physiological thresholds but are a complex
563 function of the assumed soil textural properties. Those properties are translated into soil hydraulic parameters
564 (Van Looy *et al.* 2017), affecting soil moisture dynamics and ET and ultimately their interplay with the value of
565 the β factor. It is currently impossible or very difficult to identify which model is more realistic in this respect
566 and each model can only “tune” all the above components at once. Specialized experiments measuring e.g.
567 simultaneously high frequency water and carbon fluxes, soil moisture and plant water status in controlled
568 environments could be designed to develop more informed parameterizations of β , and eventually expand to
569 more detailed mechanistic representation of ecosystem scale plant hydraulics (Anderegg *et al.*, 2016; Konings
570 and Gentine, 2017).

571 Correct modelling of leaf area dynamics is equally important as the plant physiological stress β for quantifying
572 the effect of rainfall changes in ecosystem functioning (Yang *et al.*, 2018). Simulation of LAI could be
573 constrained better than currently done with available information, considering that high frequency LAI
574 measurements in an experiment could be added with a relatively low budget. Observations of LAI, via indirect
575 methods, are common at large scale. Extensive ground (Iio *et al.*, 2014) and remote sensing estimates (Zhu *et*
576 *al.*, 2013) of LAI and phenology data from low cost cameras worldwide (Klosterman *et al.*, 2014; Brown *et al.*,
577 2016) can be used to further constrain phenology and carbon allocation. Regarding carbon allocation, below
578 ground dynamics and their responses to water limitation should also be simultaneously quantified.

579 From an observational perspective, in order to improve models, we need to disentangle the effects on plant
580 physiological stress from those on vegetation dynamics at the local scales. Since physiological effects of water
581 stress manifest earlier than changes of LAI or carbon pools, a nearly continuous monitoring of photosynthesis,
582 evapotranspiration, leaf and soil water potentials, sap flow and leaf area index would be essential to get further
583 insights. These quantities are often observed (e.g. using eddy covariance systems, sap flow sensors, leaf
584 porometers, hyperspectral cameras), but rarely in an integrated manner and associated with rainfall
585 manipulation experiments. This should become a priority to foster model developments.

586 Finally, new streams of data via remote sensing can be also used for detailed model confirmation at larger
587 scales. Satellite and airborne data related to vegetation structure, spanning from leaf chemistry to delineation of
588 individual trees (Andersen, *et al.*, 2006; Gougeon and Leckie, 2006; Asner and Martin, 2009), high frequency
589 photosynthesis through solar induced fluorescence (SIF), soil moisture (Liu *et al.*, 2011), and plant hydraulic
590 status (Konings and Gentine, 2017) currently exist. Such data can help us to identify the mechanistic link
591 between plant water stress and how it affects vegetation productivity from short term photosynthesis reduction
592 to decadal scales involving plant mortality and composition shifts. Note however that estimates of
593 photosynthetic activity during water stress purely based on remote sensing (light reflection signals) are often
594 biased and need to be interpreted with care (De Kauwe *et al.*, 2016; Stocker *et al.*, 2019).

595 In conclusion, our key finding in this study is that current generation terrestrial biosphere models have major
596 uncertainties related to simulating plant water stress, and its impact on the terrestrial carbon cycling. Those
597 uncertainties arise from the model formulations related to both carbon allocation patterns and phenology and
598 the representation of water stress frequency and magnitude on carbon assimilation. These two effects are
599 inherently coupled at a wide range of scales. To decouple the two effects and constrain mechanistic
600 representations of how water stress acts on multiple processes will require the close collaboration between
601 experimentalists and modellers, for planning and implementing new “high frequency” experiments (Rineau *et*
602 *al.*, 2019). These experiments should observe across a range of temporal scales from hourly values of
603 photosynthesis and ET, to daily and weekly LAI dynamics, up to arrive to annual changes in species
604 composition (Halbritter *et al.*, 2019).

605 *The authors declare no conflict of interest*

606 **Data Sharing and Accessibility statement:** All meteorological input data and model outputs can be found at
607 the zenodo data repository (<https://zenodo.org/doi:10.5281/zenodo.3627959>)

608 **Acknowledgements**

609 We would like to thank Prof. Gil Bohrer and three anonymous reviewers for their constructive comments that
610 help us improve the manuscript. A.P. acknowledges financial support from NERC (grant no. NE/S003495/1).
611 J.Z. acknowledges the Swiss National Science Foundation (Ambizione Grant 179876). DSG, PC, WL, ME, RO
612 and JP are funded by the “IMBALANCE-P” project of the European Research Council (ERC-2013-SyG-
613 610028). CP acknowledges the financial support from the Natural Sciences and Engineering Research Council
614 of Canada (NSERC) Discover Grant. YPW acknowledges the financial support from the National

615 Environmental Science Program for Earth System and Climate Change from the Australian Federal
616 government. IKS and KSL acknowledge the financial support to the CLIMAITE project at Brandbjerg from the
617 Villum Foundation. J.Po. was supported by the German Research Foundation's (DFG) Emmy Noether Program
618 (PO 1751/1-1). L.B. was supported by the DFG's CE-LAND project. Computational resources were made
619 available by the German Climate Computing Center (DKRZ) through support from the German Federal
620 Ministry of Education and Research (BMBF). MB acknowledges the support of the Austrian Science Fund
621 (FWF; P22214-B17), and the European Community's Seventh Framework Programme (FP7/2007-2013,
622 project 'CARBO-Extreme', grant agreement no. 226701), the Austrian Academy of Sciences (OeAW;
623 ClimLUC) and the Austrian Research Promotion Agency (FFG; LTER-CWN). We thank all site operators,
624 MODIS and FLUXNET2015 for providing the data for this study.

References

- Ahlström, A. *et al.* (2015) 'The dominant role of semi-arid ecosystems in the trend and variability of the land CO₂ sink', *Science*, 348(6237), pp. 895–899. doi: 10.1126/science.aaa1668.
- Alexander, L. V. *et al.* (2006) 'Global observed changes in daily climate extremes of temperature and precipitation', *Journal of Geophysical Research*, 111(D5), p. D05109. doi: 10.1029/2005JD006290.
- Allan, R. P. *et al.* (2014) 'Physically Consistent Responses of the Global Atmospheric Hydrological Cycle in Models and Observations', *Surveys in Geophysics*, 35(3), pp. 533–552. doi: 10.1007/s10712-012-9213-z.
- Allen, C. D. *et al.* (2010) 'A global overview of drought and heat-induced tree mortality reveals emerging climate change risks for forests', *Forest Ecology and Management*, 259(4), pp. 660–684. doi: 10.1016/j.foreco.2009.09.001.
- Allen, C. D., Breshears, D. D. and McDowell, N. G. (2015) 'On underestimation of global vulnerability to tree mortality and forest die-off from hotter drought in the Anthropocene', *Ecosphere*, 6(8), p. art129. doi: 10.1890/ES15-00203.1.
- Anderegg, W. R. L. *et al.* (2015) 'Pervasive drought legacies in forest ecosystems and their implications for carbon cycle models', *Science*, 349(6247), pp. 528–531. doi: 10.1126/science.aab1833.
- Anderegg, W. R. L. *et al.* (2016) 'Meta-analysis reveals that hydraulic traits explain cross-species patterns of drought-induced tree mortality across the globe', *Proceedings of the National Academy of Sciences*, 113(18), pp. 5024–5029. doi: 10.1073/pnas.1525678113.
- Andersen, H.-E., Reutebuch, S. E. and McGaughey, R. J. (2006) 'A rigorous assessment of tree height measurements obtained using airborne lidar and conventional field methods', *Canadian Journal of Remote Sensing*, 32(5), pp. 355–366. doi: 10.5589/m06-030.
- Asner, G. P. and Martin, R. E. (2009) 'Airborne spectranomics: mapping canopy chemical and taxonomic diversity in tropical forests', *Frontiers in Ecology and the Environment*, 7(5), pp. 269–276. doi: 10.1890/070152.
- Babst, F. *et al.* (2018) 'When tree rings go global: Challenges and opportunities for retro- and prospective insight', *Quaternary Science Reviews*, 197, pp. 1–20. doi: 10.1016/j.quascirev.2018.07.009.

Báez, S. *et al.* (2013) 'Effects of experimental rainfall manipulations on Chihuahuan Desert grassland and shrubland plant communities', *Oecologia*, 172(4), pp. 1117–1127. doi: 10.1007/s00442-012-2552-0.

Beier, C. *et al.* (2009) 'Carbon and nitrogen balances for six shrublands across Europe', *Global Biogeochemical Cycles*, 23(4), p. n/a-n/a. doi: 10.1029/2008GB003381.

Bonan, G. B. *et al.* (2014) 'Modeling stomatal conductance in the Earth system: linking leaf water-use efficiency and water transport along the soil-plant-atmosphere continuum', *Geoscientific Model Development*, 7(3), pp. 3085–3159. doi: 10.5194/gmd-7-2193-2014.

Brown, T. B. *et al.* (2016) 'Using phenocams to monitor our changing Earth: toward a global phenocam network', *Frontiers in Ecology and the Environment*, 14(2), pp. 84–93. doi: 10.1002/fee.1222.

Choat, B. *et al.* (2012) 'Global convergence in the vulnerability of forests to drought', *Nature*, 491(7426), pp. 752–755. doi: 10.1038/nature11688.

Clark, D. B. *et al.* (2011) 'The Joint UK Land Environment Simulator (JULES), model description – Part 2: Carbon fluxes and vegetation dynamics', *Geoscientific Model Development*, 4(3), pp. 701–722. doi: 10.5194/gmd-4-701-2011.

Collins, S. L. *et al.* (2012) 'Stability of tallgrass prairie during a 19-year increase in growing season precipitation', *Functional Ecology*, 26(6), pp. 1450–1459. doi: 10.1111/j.1365-2435.2012.01995.x.

Dietze, M. C., *et al.*, (2011). Characterizing the performance of ecosystem models across time scales: A spectral analysis of the North American Carbon Program site-level synthesis. *Journal of Geophysical Research*, 116(G4), G04029. <https://doi.org/10.1029/2011JG001661>

Egea, G., Verhoef, A. and Vidale, P. L. (2011) 'Towards an improved and more flexible representation of water stress in coupled photosynthesis–stomatal conductance models', *Agricultural and Forest Meteorology*. Elsevier B.V., 151(10), pp. 1370–1384. doi: 10.1016/j.agrformet.2011.05.019.

Eller, C. B. *et al.* (2018) 'Modelling tropical forest responses to drought and El Niño with a stomatal optimization model based on xylem hydraulics', *Philosophical Transactions of the Royal Society B: Biological Sciences*, 373(1760), p. 20170315. doi: 10.1098/rstb.2017.0315.

Estiarte, M. *et al.* (2016) 'Few multiyear precipitation-reduction experiments find a shift in the productivity-precipitation relationship', *Global change biology*, 22(7), pp. 2570–2581. doi: 10.1111/gcb.13269.

Fang, H. *et al.* (2013) 'Characterization and intercomparison of global moderate resolution leaf area index (LAI) products: Analysis of climatologies and theoretical uncertainties', *Journal of Geophysical Research: Biogeosciences*, 118(2), pp. 529–548. doi: 10.1002/jgrg.20051.

Fatichi, S. *et al.* (2019) 'Modelling carbon sources and sinks in terrestrial vegetation', *New Phytologist*, 221(2), pp. 652–668. doi: 10.1111/nph.15451.

Fatichi, S. and Ivanov, V. Y. (2014) 'Interannual variability of evapotranspiration and vegetation productivity', *Water Resources Research*, 50(4), pp. 3275–3294. doi: 10.1002/2013WR015044.

Fatichi, S., Ivanov, V. Y. and Caporali, E. (2012) 'A mechanistic ecohydrological model to investigate complex interactions in cold and warm water-controlled environments: 1. Theoretical framework and plot-scale analysis', *Journal of Advances in Modeling Earth Systems*, 4(2), p. n/a-n/a. doi: 10.1029/2011MS000086.

Fatichi, S. and Leuzinger, S. (2013) 'Reconciling observations with modeling: The fate of water and carbon allocation in a mature deciduous forest exposed to elevated CO₂', *Agricultural and Forest Meteorology*. Elsevier B.V., 174–175, pp. 144–157. doi: 10.1016/j.agrformet.2013.02.005.

Fatichi, S., Pappas, C. and Ivanov, V. Y. (2016) 'Modeling plant-water interactions: an ecohydrological overview from the cell to the global scale', *Wiley Interdisciplinary Reviews: Water*, 3(3), pp. 327–368. doi: 10.1002/wat2.1125.

Fay, P. a. *et al.* (2008) 'Changes in grassland ecosystem function due to extreme rainfall events: implications for responses to climate change', *Global Change Biology*, 14(7), pp. 1600–1608. doi: 10.1111/j.1365-2486.2008.01605.x.

Fisher, R. A. *et al.* (2007) 'The response of an Eastern Amazonian rain forest to drought stress: results and modelling analyses from a throughfall exclusion experiment', *Global Change Biology*, 13(11), pp. 2361–2378. doi: 10.1111/j.1365-2486.2007.01417.x.

Frank, D. D. *et al.* (2015) 'Effects of climate extremes on the terrestrial carbon cycle: concepts, processes and potential future impacts', *Global Change Biology*, 21(January), pp. 2861–2880. doi: 10.1111/gcb.12916.

Fuchslueger, L. *et al.* (2014) 'Experimental drought reduces the transfer of recently fixed plant carbon to soil microbes and alters the bacterial community composition in a mountain meadow', *New Phytologist*, 201(3), pp. 916–927. doi: 10.1111/nph.12569.

Gentine, P., et al, (2019), Land–atmosphere interactions in the tropics – a review, *Hydrol. Earth Syst. Sci.*, 23, 4171–4197, doi: 10.5194/hess-23-4171-2019, 2019.

Goll, D. S. *et al.* (2017) ‘A representation of the phosphorus cycle for ORCHIDEE (revision 4520)’, *Geoscientific Model Development*, 10(10), pp. 3745–3770. doi: 10.5194/gmd-10-3745-2017.

Golodets, C. *et al.* (2013) ‘From desert to Mediterranean rangelands: will increasing drought and inter-annual rainfall variability affect herbaceous annual primary productivity?’, *Climatic Change*, 119(3–4), pp. 785–798. doi: 10.1007/s10584-013-0758-8.

Golodets, C. *et al.* (2015) ‘Climate change scenarios of herbaceous production along an aridity gradient: vulnerability increases with aridity’, *Oecologia*, 177(4), pp. 971–979. doi: 10.1007/s00442-015-3234-5.

Gougeon, F. A. and Leckie, D. G. (2006) ‘The Individual Tree Crown Approach Applied to Ikonos Images of a Coniferous Plantation Area’, *Photogrammetric Engineering & Remote Sensing*, 72(11), pp. 1287–1297. doi: 10.14358/PERS.72.11.1287.

Goward, S. N. and Prince, S. D. (1995) ‘Transient Effects of Climate on Vegetation Dynamics: Satellite Observations’, *Journal of Biogeography*, 22(2/3), p. 549. doi: 10.2307/2845953.

Green, J. K. *et al.* (2017) ‘Regionally strong feedbacks between the atmosphere and terrestrial biosphere’, *Nature Geoscience*, 10(6), pp. 410–414. doi: 10.1038/ngeo2957.

Green, J. K. *et al.* (2019) ‘Large influence of soil moisture on long-term terrestrial carbon uptake’, *Nature*. Springer US, 565(7740), pp. 476–479. doi: 10.1038/s41586-018-0848-x.

Hagedorn F. *et al.* (2016), Recovery of trees from drought depends on belowground sink control, *Nature Plants*, 2 (16111), doi: 10.1038/nplants.2016.111.

Halbritter A. H. *et al.*, (2019) The handbook for standardized field and laboratory measurements in terrestrial climate change experiments and observational studies (ClimEx), *Methods in Ecology and Evolution*, doi: 10.1111/2041-210X.13331

Hanson, P. J. *et al.* (2004) ‘Oak forest carbon and water simulations: model intercomparisons and evaluations against independent data’, *Ecological Monographs*, 74(3), pp. 443–489. doi: 10.1890/03-4049.

Hanson, P. J. and Wullschleger, S. D. (eds) (2003) *North American Temperate Deciduous Forest Responses to*

Changing Precipitation Regimes. New York, NY: Springer New York (Ecological Studies). doi: 10.1007/978-1-4613-0021-2.

Hasibeder R. *et al.*, (2014), Summer drought alters carbon allocation to roots and root respiration in mountain grassland, *New Phytologist*, 205(3), 1117-1127, doi: 10.1111/nph.13146

Heisler-White, J. L. *et al.* (2009) 'Contingent productivity responses to more extreme rainfall regimes across a grassland biome', *Global Change Biology*, 15(12), pp. 2894–2904. doi: 10.1111/j.1365-2486.2009.01961.x.

Heisler-White, J. L., Knapp, A. K. and Kelly, E. F. (2008) 'Increasing precipitation event size increases aboveground net primary productivity in a semi-arid grassland.', *Oecologia*, 158(1), pp. 129–140. doi: 10.1007/s00442-008-1116-9.

Hu, Z. *et al.* (2018) 'Joint structural and physiological control on the interannual variation in productivity in a temperate grassland: A data-model comparison', *Global Change Biology*, 24(7), pp. 2965–2979. doi: 10.1111/gcb.14274.

Huang Y., *et al.*, (2017), Soil thermal dynamics, snow cover, and frozen depth under five temperature treatments in an ombrotrophic bog: Constrained forecast with data assimilation, *Journal of Geophysical Research: Biogeosciences*, 122(8), doi: 10.1002/2016JG003725.

Humphrey, V. *et al.* (2018) 'Sensitivity of atmospheric CO₂ growth rate to observed changes in terrestrial water storage', *Nature*. Springer US, 560(7720), pp. 628–631. doi: 10.1038/s41586-018-0424-4.

Huxman, T. E. *et al.* (2004) 'Precipitation pulses and carbon fluxes in semiarid and arid ecosystems.', *Oecologia*, 141(2), pp. 254–268. doi: 10.1007/s00442-004-1682-4.

Iio, A. *et al.* (2014) 'Global dependence of field-observed leaf area index in woody species on climate: a systematic review', *Global Ecology and Biogeography*, 23(3), pp. 274–285. doi: 10.1111/geb.12133.

IPCC (2012) *Managing the Risks of Extreme Events and Disasters to Advance Climate Change Adaptation*. Edited by C. B. Field *et al.* Cambridge Univ Press.

IPCC (2013) *Climate Change 2013: The Physical Science Basis. Contribution of Working Group I to the Fifth Assessment Report of the Intergovernmental Panel on Climate Change*. Cambridge University Press Cambridge, UK.

Jarvis P. et al., (2007), Drying and wetting of Mediterranean soils stimulates decomposition and carbon dioxide emission: the “Birch effect”, *Tree Physiology*, 27(7), 929-940, doi: 10.1093/treephys/27.7.929

Kaminski, T. et al. (2013) ‘The BETHY/JSBACH Carbon Cycle Data Assimilation System: experiences and challenges’, *Journal of Geophysical Research: Biogeosciences*, 118(4), pp. 1414–1426. doi: 10.1002/jgrg.20118.

De Kauwe, M. G. et al. (2013) ‘Forest water use and water use efficiency at elevated CO₂: a model-data intercomparison at two contrasting temperate forest FACE sites.’, *Global change biology*, 19(6), pp. 1759–1779. doi: 10.1111/gcb.12164.

De Kauwe, M. G., Kala, J., et al. (2015) ‘A test of an optimal stomatal conductance scheme within the CABLE land surface model’, *Geoscientific Model Development*, 8(2), pp. 431–452. doi: 10.5194/gmd-8-431-2015.

De Kauwe, M. G., Zhou, S.-X. X., et al. (2015) ‘Do land surface models need to include differential plant species responses to drought? Examining model predictions across a mesic-xeric gradient in Europe’, *Biogeosciences Discussions*, 12(24), pp. 7503–7518. doi: 10.5194/bgd-12-12349-2015.

De Kauwe, M. G. et al. (2016) ‘Satellite based estimates underestimate the effect of CO₂ fertilization on net primary productivity’, *Nature Climate Change*. Nature Publishing Group, 6(10), pp. 892–893. doi: 10.1038/nclimate3105.

De Kauwe, M. G. et al. (2017) ‘Challenging terrestrial biosphere models with data from the long-term multifactor Prairie Heating and CO₂ Enrichment experiment’, *Global Change Biology*, 23(9), pp. 3623–3645. doi: 10.1111/gcb.13643.

Kayler Z. E., et al., (2015). Experiments to Confront the Environmental Extremes of Climate Change. *Frontiers in Ecology and the Environment*, 13(4), 219-225, doi: 10.1890/140174

Kennedy, D. et al. (2019) ‘Implementing Plant Hydraulics in the Community Land Model, Version 5’, *Journal of Advances in Modeling Earth Systems*, 11(2), pp. 485–513. doi: 10.1029/2018MS001500.

Klein, T. et al. (2014) ‘Towards an advanced assessment of the hydrological vulnerability of forests to climate change-induced drought’, *New Phytologist*, 201(3), pp. 712–716. doi: 10.1111/nph.12548.

Klosterman, S. T. et al. (2014) ‘Evaluating remote sensing of deciduous forest phenology at multiple spatial scales using PhenoCam imagery’, *Biogeosciences*, 11(16), pp. 4305–4320. doi: 10.5194/bg-11-4305-2014.

Knapp, A. K. and Smith, M. D. (2001) 'Variation among biomes in temporal dynamics of aboveground primary production.', *Science*, 291(5503), pp. 481–484. doi: 10.1126/science.291.5503.481.

Knutti, R. and Sedláček, J. (2013) 'Robustness and uncertainties in the new CMIP5 climate model projections', *Nature Climate Change*, 3(4), pp. 369–373. doi: 10.1038/nclimate1716.

Kongstad, J. *et al.* (2012) 'High Resilience in Heathland Plants to Changes in Temperature, Drought, and CO₂ in Combination: Results from the CLIMAITE Experiment', *Ecosystems*, 15(2), pp. 269–283. doi: 10.1007/s10021-011-9508-9.

Konings, A. G. and Gentine, P. (2017) 'Global variations in ecosystem-scale isohydricity', *Global Change Biology*, 23(2), pp. 891–905. doi: 10.1111/gcb.13389.

Körner, C. (2019) 'No need for pipes when the well is dry—a comment on hydraulic failure in trees', *Tree Physiology*. Edited by S. Sevanto, pp. 1–6. doi: 10.1093/treephys/tpz030.

Koster, R. D. (2004) 'Regions of Strong Coupling Between Soil Moisture and Precipitation', *Science*, 305(5687), pp. 1138–1140. doi: 10.1126/science.1100217.

Krinner, G. *et al.* (2005) 'A dynamic global vegetation model for studies of the coupled atmosphere-biosphere system', *Global Biogeochemical Cycles*, 19(1). doi: 10.1029/2003GB002199.

Lawrence, D. M., *et al.*, (2019). The Community Land Model version 5: Description of new features, benchmarking, and impact of forcing uncertainty. *Journal of Advances in Modeling Earth Systems*, 11. <https://doi.org/10.1029/2018MS001583>

Lemordant, L. *et al.* (2016) 'Modification of land-atmosphere interactions by CO₂ effects: Implications for summer dryness and heat wave amplitude', *Geophysical Research Letters*, 43(19), pp. 10,240–10,248. doi: 10.1002/2016GL069896.

Lienert, S. and Joos, F. (2018) 'A Bayesian ensemble data assimilation to constrain model parameters and land-use carbon emissions', *Biogeosciences*, 15(9), pp. 2909–2930. doi: 10.5194/bg-15-2909-2018.

Limousin, J. M. *et al.*, (2009), Long-term transpiration change with rainfall decline in a Mediterranean Quercus ilex forest. *Global Change Biology*, 15(9), 2163–2175, doi: 10.1111/j.1365-2486.2009.01852.x

Liu, Y. Y. *et al.* (2011) 'Developing an improved soil moisture dataset by blending passive and active

microwave satellite-based retrievals', *Hydrology and Earth System Sciences*, 15(2), pp. 425–436. doi: 10.5194/hess-15-425-2011.

Van Looy, K. *et al.* (2017) 'Pedotransfer Functions in Earth System Science: Challenges and Perspectives', *Reviews of Geophysics*, 55(4), pp. 1199–1256. doi: 10.1002/2017RG000581.

Manzoni, S. *et al.* (2013) 'Biological constraints on water transport in the soil–plant–atmosphere system', *Advances in Water Resources*, 51, pp. 292–304. doi: 10.1016/j.advwatres.2012.03.016.

Matheny, A. M., *et al.*, (2014). Characterizing the diurnal patterns of errors in the prediction of evapotranspiration by several land-surface models: An NACP analysis. *Journal of Geophysical Research: Biogeosciences*, 119(7), 1458–1473. <https://doi.org/10.1002/2014JG002623>

Martin-Stpaul, N. K. *et al.* (2013) 'The temporal response to drought in a Mediterranean evergreen tree: Comparing a regional precipitation gradient and a throughfall exclusion experiment', *Global Change Biology*, 19(8), pp. 2413–2426. doi: 10.1111/gcb.12215.

Mauritsen T., *et al.*, (2019), Developments in the MPI-M Earth System Model version 1.2 (MPI-ESM1.2) and Its Response to Increasing CO₂, *Journal of Advances in Modeling Earth Systems*, 11(4), doi: 10.1029/2018MS001400.

McDowell, N. G. (2011) 'Mechanisms linking drought, hydraulics, carbon metabolism, and vegetation mortality.', *Plant physiology*, 155(3), pp. 1051–1059. doi: 10.1104/pp.110.170704.

McDowell, N. G. *et al.* (2013) 'Evaluating theories of drought-induced vegetation mortality using a multimodel-experiment framework', *New Phytologist*, 200(2), pp. 304–321. doi: 10.1111/nph.12465.

Medlyn, B. E. *et al.* (2015) 'Using ecosystem experiments to improve vegetation models', *Nature Climate Change*. Nature Publishing Group, 5(6), pp. 528–534. doi: 10.1038/nclimate2621.

Medlyn, B. E., De Kauwe, M. G. and Duursma, R. A. (2016a) 'New developments in the effort to model ecosystems under water stress', *New Phytologist*, 212(1), pp. 5–7. doi: 10.1111/nph.14082.

Medlyn, B. E., *et al.*, (2016b). Using models to guide field experiments: a priori predictions for the CO₂ response of a nutrient- and water-limited native Eucalypt woodland. *Global Change Biology*, 22(8), 2834–2851. <https://doi.org/10.1111/gcb.13268>

Miralles, D. G. *et al.* (2018) 'Land-atmospheric feedbacks during droughts and heatwaves: state of the science and current challenges', *Annals of the New York Academy of Sciences*, 1436, pp. 19–35. doi: 10.1111/nyas.13912.

Miranda, J. D. *et al.* (2011) 'Climatic change and rainfall patterns: Effects on semi-arid plant communities of the Iberian Southeast', *Journal of Arid Environments*. Elsevier Ltd, 75(12), pp. 1302–1309. doi: 10.1016/j.jaridenv.2011.04.022.

Mirfenderesgi, G. *et al.* (2016) 'Tree level hydrodynamic approach for resolving aboveground water storage and stomatal conductance and modeling the effects of tree hydraulic strategy', *Journal of Geophysical Research: Biogeosciences*, 121(7), pp. 1792–1813. doi: 10.1002/2016JG003467.

Nepstad, D. C., *et al.*, (2007). Mortality of large trees and lianas following experimental drought in an amazon forest. *Ecology*, 88(9), 2259–2269. <https://doi.org/10.1890/06-1046.1>

Ogaya, R. and Peñuelas, J. (2007) 'Tree growth, mortality, and above-ground biomass accumulation in a holm oak forest under a five-year experimental field drought', *Plant Ecology*, 189(2), pp. 291–299. doi: 10.1007/s11258-006-9184-6.

Pappas C. *et al.*, (2017) Ecosystem functioning is enveloped by hydrometeorological variability. *Nature ecology & evolution*, 1(9), 1263, doi: 10.1038/s41559-017-0277-5.

Paschalis, A. *et al.* (2015) 'Cross-scale impact of climate temporal variability on ecosystem water and carbon fluxes', *Journal of Geophysical Research: Biogeosciences*, 120(9), pp. 1716–1740. doi: 10.1002/2015JG003002.

Paschalis, A. *et al.* (2017) 'On the variability of the ecosystem response to elevated atmospheric CO₂ across spatial and temporal scales at the Duke Forest FACE experiment', *Agricultural and Forest Meteorology*. Elsevier B.V., 232, pp. 367–383. doi: 10.1016/j.agrformet.2016.09.003.

Peñuelas, J. *et al.* (2004) 'Complex spatiotemporal phenological shifts as a response to rainfall changes', *New Phytologist*, 161(3), pp. 837–846. doi: 10.1111/j.1469-8137.2004.01003.x.

Poulter, B. *et al.* (2014) 'Contribution of semi-arid ecosystems to interannual variability of the global carbon cycle', *Nature*. Nature Publishing Group, 509(7502), pp. 600–603. doi: 10.1038/nature13376.

Powell, T. L. *et al.* (2013) 'Confronting model predictions of carbon fluxes with measurements of Amazon

forests subjected to experimental drought', *New Phytologist*, 200(2), pp. 350–365. doi: 10.1111/nph.12390.

Le Quéré, C. *et al.* (2018) 'Global Carbon Budget 2018', *Earth System Science Data*, 10(4), pp. 2141–2194. doi: 10.5194/essd-10-2141-2018.

Reichstein, M. *et al.* (2013) 'Climate extremes and the carbon cycle.', *Nature*. Nature Publishing Group, 500(7462), pp. 287–295. doi: 10.1038/nature12350.

Richardson, A. D., *et al.*, (2012). Terrestrial biosphere models need better representation of vegetation phenology: results from the North American Carbon Program Site Synthesis. *Global Change Biology*, 18(2), 566–584. doi: 10.1111/j.1365-2486.2011.02562.x

Rineau F. *et al.*, (2019) Towards more predictive and interdisciplinary climate change ecosystem experiments, *Nature Climate Change*, 9. 809-819, doi: 10.1038/s41558-019-0609-3.

Ross I. *et al.*, (2012), How do variations in the temporal distribution of rainfall events affect ecosystem fluxes in seasonally water-limited Northern Hemisphere shrublands and forests?, *Biogeosciences* 9(9):1007-1024, doi: 10.5194/bg-9-1007-2012.

Rowland, L., *et al.*, (2014). Evidence for strong seasonality in the carbon storage and carbon use efficiency of an Amazonian forest. *Global Change Biology*, 20(3), 979–991. <https://doi.org/10.1111/gcb.12375>

Seneviratne, S. I. *et al.* (2013) 'Impact of soil moisture-climate feedbacks on CMIP5 projections: First results from the GLACE-CMIP5 experiment', *Geophysical Research Letters*, 40(19), pp. 5212–5217. doi: 10.1002/grl.50956.

Stocker, B. D. *et al.* (2019) 'Drought impacts on terrestrial primary production underestimated by satellite monitoring', *Nature Geoscience*. Springer US, 12(4), pp. 264–270. doi: 10.1038/s41561-019-0318-6.

Stuart-Haëntjens E., *et al.*, (2018), Mean annual precipitation predicts primary production resistance and resilience to extreme drought, *Science of the total Environment*, 636(15), 360-366, doi: 10.1016/j.scitotenv.2018.04.290.

Taylor, K. E. (2001) 'Summarizing multiple aspects of model performance in a single diagram', *Journal of Geophysical Research*, 106(D7), pp. 7183–7192. doi: 10.1029/2000JD900719.

Thurner, M. *et al.* (2017) 'Evaluation of climate-related carbon turnover processes in global vegetation models

for boreal and temperate forests', *Global Change Biology*, 23(8), pp. 3076–3091. doi: 10.1111/gcb.13660.

Tian, H. *et al.* (2010) 'Model estimates of net primary productivity, evapotranspiration, and water use efficiency in the terrestrial ecosystems of the southern United States during 1895–2007', *Forest Ecology and Management*, 259(7), pp. 1311–1327. doi: 10.1016/j.foreco.2009.10.009.

Tielbörger, K. *et al.* (2014) 'Middle-Eastern plant communities tolerate 9 years of drought in a multi-site climate manipulation experiment', *Nature Communications*, 5(1), p. 5102. doi: 10.1038/ncomms6102.

Trugman, A. T., *et al.* (2018). Soil Moisture Stress as a Major Driver of Carbon Cycle Uncertainty. *Geophysical Research Letters*, 45(13), 6495–6503. doi: 10.1029/2018GL078131

Ukkola, A. M. *et al.* (2016) 'Land surface models systematically overestimate the intensity, duration and magnitude of seasonal-scale evaporative droughts', *Environmental Research Letters*. IOP Publishing, 11(10), p. 104012. doi: 10.1088/1748-9326/11/10/104012.

Vicca, S. *et al.*, (2012), Urgent need for a common metric to make precipitation manipulation experiments comparable, *New Phytologist*, 195(3), 518-522, doi: 10.1111/j.1469-8137.2012.04224.x

Vicca, S. *et al.* (2014) 'Can current moisture responses predict soil CO₂ efflux under altered precipitation regimes? A synthesis of manipulation experiments', *Biogeosciences*, 11(11), pp. 2991–3013. doi: 10.5194/bg-11-2991-2014.

Vicca, S. *et al.*, (2016) Remotely-sensed detection of effects of extreme droughts on gross primary production, *Scientific Reports*, 6(28269), doi: 10.1038/srep28269

Walker, A. P. *et al.* (2014) 'Comprehensive ecosystem model-data synthesis using multiple data sets at two temperate forest free-air CO₂ enrichment experiments: Model performance at ambient CO₂ concentration', *Journal of Geophysical Research: Biogeosciences*, 119(5), pp. 937–964. doi: 10.1002/2013JG002553.

Wang, Y. P. *et al.* (2011) 'Diagnosing errors in a land surface model (CABLE) in the time and frequency domains', *Journal of Geophysical Research*, 116(G1), p. G01034. doi: 10.1029/2010JG001385.

Wu, D. *et al.* (2018) 'Asymmetric responses of primary productivity to altered precipitation simulated by ecosystem models across three long-term grassland sites', *Biogeosciences*, 15(11), pp. 3421–3437. doi: 10.5194/bg-15-3421-2018.

- Xu, C. *et al.* (2013) 'Our limited ability to predict vegetation dynamics under water stress', *New Phytologist*, 200(2), pp. 298–300. doi: 10.1111/nph.12450.
- Xu, X. *et al.* (2016) 'Diversity in plant hydraulic traits explains seasonal and inter-annual variations of vegetation dynamics in seasonally dry tropical forests', *New Phytologist*, 212(1), pp. 80–95. doi: 10.1111/nph.14009.
- Yang, J. *et al.* (2018) 'Applying the Concept of Ecohydrological Equilibrium to Predict Steady State Leaf Area Index', *Journal of Advances in Modeling Earth Systems*, 10(8), pp. 1740–1758. doi: 10.1029/2017MS001169.
- Zaehle, S. *et al.* (2014) 'Evaluation of 11 terrestrial carbon-nitrogen cycle models against observations from two temperate Free-Air CO₂ Enrichment studies', *New Phytologist*, 202(3), pp. 803–822. doi: 10.1111/nph.12697.
- Zhang, W. *et al.* (2019) 'Ecosystem structural changes controlled by altered rainfall climatology in tropical savannas', *Nature Communications*. Springer US, 10(1), p. 671. doi: 10.1038/s41467-019-08602-6.
- Zhao, M. and Running, S. W. (2010) 'Drought-Induced Reduction in Global Terrestrial Net Primary Production from 2000 Through 2009', *Science*, 329(5994), pp. 940–943. doi: 10.1126/science.1192666.
- Zhou, S. *et al.* (2013) 'How should we model plant responses to drought? An analysis of stomatal and non-stomatal responses to water stress', *Agricultural and Forest Meteorology*. Elsevier B.V., 182–183, pp. 204–214. doi: 10.1016/j.agrformet.2013.05.009.
- Zhu, Z. *et al.* (2013) 'Global Data Sets of Vegetation Leaf Area Index (LAI)_{3g} and Fraction of Photosynthetically Active Radiation (FPAR)_{3g} Derived from Global Inventory Modeling and Mapping Studies (GIMMS) Normalized Difference Vegetation Index (NDVI)_{3g} for the Period 1981 to 2012', *Remote Sensing*, 5(2), pp. 927–948. doi: 10.3390/rs5020927.
- Zscheischler, J., Mahecha, M. D., *et al.* (2014a) 'A few extreme events dominate global interannual variability in gross primary production', *Environmental Research Letters*, 9(3), p. 035001. doi: 10.1088/1748-9326/9/3/035001.
- Zscheischler, J., Michalak, A. M., *et al.* (2014b) 'Impact of large-scale climate extremes on biospheric carbon fluxes: An intercomparison based on MsTMIP data', *Global Biogeochemical Cycles*, 28(6), pp. 585–600. doi: 10.1002/2014GB004826.

Zscheischler, J. *et al.* (2016) 'Short-term favorable weather conditions are an important control of interannual variability in carbon and water fluxes', *Journal of Geophysical Research: Biogeosciences*, 121(8), pp. 2186–2198. doi: 10.1002/2016JG003503.

Accepted Article